

Centro de Previsão de Tempo e Estudos Climáticos (CPTEC), Instituto Nacional de Pesquisas Espaciais (INPE), São José dos Campos, SP, Brazil

**EXPERIMENTS WITH EOF-BASED PERTURBATION AND BREEDING
OF GROWING MODES METHODS AND THEIR IMPACTS ON
CPTEC/INPE ENSEMBLE PREDICTION SYSTEM**

Antônio Marcos Mendonça and José Paulo Bonatti

With 18 Figures

Summary

The impact of modifications in the perturbation method based on empirical orthogonal functions (EOF-method, Zhang and Krishnamurti, 1999) used operationally on the ensemble prediction system (EPS) at CPTEC/INPE is evaluated. The main changes proposed in this study are: application of EOF-method to perturb the midlatitudes; application of additional perturbations on the surface pressure (P) and specific humidity (Q) fields; selection of most unstable perturbations based on the linear growth rate of EOF coefficients; to use a simplified version of the breeding of growing modes method (Toth and Kalnay, 1993) for generating perturbed initial conditions. The impacts of these modifications are evaluated under the hypothesis of perfect model for both an operational suite during January 2005 and a case study for the first documented hurricane over South Atlantic, occurred in March 2004. The statistical indexes used to evaluate the results are pattern anomaly correlation, root mean square error, ensemble spread, brier skill score and perturbation versus error correlation analysis (PECA). Results indicate that applying simultaneously additional perturbations in both the extratropics and on P and Q fields contributes to improve the performance of CPTEC-EPS and to enhance the quality of forecast perturbations. Moreover, initial EOF-perturbations computed over South America have positive impacts on the ensemble forecasts over South America, according to both evaluations: operational suite and in the hurricane case study. Despite simplifications, the simplified breeding method presents competitive results in global scales, but locally it is slightly worse, due, in part, to the lack of regional rescaling.

1. Introduction

Atmospheric forecasts with high skill are an objective and at the same time a challenge to numerical weather prediction. In order to increase the quality of the numerical weather forecasts two main factors must be taken into account: the representation of physical and dynamical processes of atmosphere by numerical models and an initial condition that reproduces realistically the atmospheric state at the beginning of model integrations. The fast development of computational technology over the last few decades provided conditions for a better representation of the physical processes observed in the atmosphere by numerical models. On the other hand, the advent of the meteorological satellite information increased significantly the amount of data for generating analyses and, in addition, improvements in the methods of data assimilation (Hamill, 2002, Kalnay et al., 2002, Rabier et al., 2000) have contributed to produce high quality analyses. However, despite the advances in representation of atmospheric processes by numerical models and production of accurate analyses, numerical forecasts diverge from observed atmospheric evolution after some days of model integration. The sources of numerical weather forecast errors are mainly the two factors described previously: deficiencies of the models in representing dynamical and physical processes of the real atmosphere, called external error; and uncertainties on the state of the atmosphere at initial time, called internal error (Reynolds et al., 1994).

The model uncertainties were considered in the development of ensemble forecasting systems that run the model a number of times with different parameterization schemes to create a set of perturbed forecasts (Krishnamurti et al., 2000 and Houtekamer et al., 1996). The model uncertainties were also treated in a method described by Buizza et al. (1999). In their scheme, the random model errors due to the physical parameterization process are simulated by including stochastic perturbations in the parameterized diabatic tendency for any component of the state vector.

The importance of the initial state uncertainties in forecast errors is explained by the theory known as *chaos* which, in a simplified form, is related to the

sensitivity that some nonlinear deterministic dynamic systems exhibit with respect to initial and boundary conditions as they evolve in time (Lorenz, 1963, 1965 and 1969). The atmosphere is an example of a chaotic system, i.e., slightly different initial conditions may lead to significantly different final solutions. Thus, even though in a perfect model scenario, since the atmospheric state is not completely represented by the analysis, the unavoidable errors will grow as the model evolves with time, degrading the quality of forecast and maintaining the impossibility of calculating the future state of the atmosphere indefinitely.

Some ensemble weather prediction systems do not take into account the uncertainties in numerical models and consider only the uncertainties in the initial conditions. In these systems, one of the most important characteristic is the strategy used to generate the perturbed analysis. Under the perfect model hypothesis, they try to estimate perturbations that have potential to grow in time and could produce a set of forecasts that are diverse enough to get an impression of the likely range of future atmospheric states (Buizza, et al., 1999).

The National Centers for Environmental Prediction (NCEP) and the European Centre for Medium-Range Weather Forecasts (ECMWF) in 1992 were the pioneer centers that implemented operational ensemble weather forecasting. They used the *breeding of growing modes* (Toth and Kalnay, 1993) and the *singular vectors* (Molteni et al., 1996) methods, respectively, to generate perturbed initial conditions. The breeding-method is based on the assumption that the fast growing modes develop naturally in a data assimilation cycle, thus the perturbations are obtained as the difference between the most recent 24-hours perturbed forecasts pair (negative and positive). These differences are scaled for specified amplitude and then added (subtracted) to (from) the control analysis to form an ensemble of initial conditions for the next ensemble forecast. The singular vectors procedure assumes that error growth is approximately linear for up to two days of forecast, and uses a linearized version of the forecast model together with its adjoint to identify the fast-growing modes through the solution of an eigenvalue problem. Several studies have discussed the characteristics and evaluated the performance of these two ensembles (Tracton and Kalnay, 1993; Whitaker and Lough, 1998; Toth and Kalnay, 1997; Buizza, 1997; Àtger, 1999, Wei and Toth, 2003; Buizza et al., 2005). Later, other methods for generating perturbed analysis and ensemble

forecasting were developed, such as the perturbed-observation approach (Houtekamer et al., 1996) and more recently, perturbation methods based on Ensemble Kalman Filter (Wei et al., 2006; Wang and Bishop, 2003; Ott et al., 2004; Bishop et al., 2001).

Zhang and Krishnamurti (1999, hereinafter ZK1999) developed a procedure for generating initial ensemble perturbations based on principal component analysis (empirical orthogonal functions - EOF) called *EOF-based perturbation* (EOF-method) in order to produce hurricane ensemble forecasting. In this method, the most unstable modes defined as *optimal perturbations* are obtained as the eigenvectors whose EOF coefficients increase rapidly with time. Their results showed that the EOF eigenmodes of the first order present that characteristic.

Coutinho (1999) performed adaptations to the EOF-method in order to produce perturbed initial conditions with the atmospheric general circulation model (AGCM) of the Center for Weather Prediction and Climate Studies / National Institute for Space Research (CPTEC/INPE). The ensemble forecasts initialized with the EOF-method presented better results when compared with ensemble predictions based on random initial perturbations. Moreover, the EOF ensemble mean forecasts presented better performance than the control forecasts. In October 2001, the CPTEC/INPE started to produce operational ensemble weather forecasting using the approach described in Coutinho (1999). In Farina et al. (2005) the EOF-method together with the CPTEC-AGCM also was used to generate perturbed surface wind stress in order to force an ocean wave model and produce ocean wave ensemble predictions.

Mendonça and Bonatti (2006) evaluated the CPTEC/INPE ensemble prediction system (EPS) using statistical indexes (anomaly correlation, root mean square (rms) error, standard deviation spread) and showed that, at least for 500-hPa geopotential height, the CPTEC/INPE ensemble forecasts have characteristics of a under-dispersive system, i.e., the ensemble spread is smaller than the rms error of the ensemble mean forecasts. As an attempt to reduce this deficiency it was suggested modifications in the region used to compute the perturbations. In the operational version, the perturbations were computed in a latitude belt between 45° S and 30° N for temperature and wind fields. They found that the application of the EOF-method to calculate additional extratropical perturbations

enhances the performance of CPTEC-EPS, mainly for the first few forecast lead times.

The influence of extratropical systems over tropical region dynamic and vice versa is known (Palmer, 1988). Some works (Mo and Higgins, 1998; Simmons, 1982; Hoskins and Karoly 1981; and others) describe the connection between anomalies in tropical atmospheric systems and the observed variability in determined extratropical regions, in several time scales. On the other hand, the propagation of transient systems from midlatitudes toward the tropics may be a source of energy to tropical systems. Liebmann and Hartmann (1984) concluded that in the scales of 5 to 10 days, mid-latitude systems exert strong influence over the tropical atmosphere. Thus, the perturbation growth in the midlatitudes may influence the quality of the forecast in the tropics through the tropic-extratropic interaction of the atmosphere. Reynolds et al. (1994) found that the random error growth in the NCEP-AGCM over the extratropics due the model dynamical instability is much greater than over the tropics. As a consequence, Zhang (1997) suggested that it would be better to generate perturbations over midlatitudes and tropics separately.

Our motivation to produce this investigation is the attempt to improve the quality of the CPTEC/INPE ensemble forecasts and show to the scientific community the current status of our ensemble prediction system. To this end, we evaluate in details the influence that the midlatitude EOF-perturbations exerts over the quality of the CPTEC/INPE ensemble forecasts in both global and local scales, especially over South America. We also investigate the impact of applying perturbations on the surface pressure and specific humidity that are prognostics fields of the model but are not perturbed in the operational version of the CPTEC-EPS. Furthermore, we investigate the performance of the CPTEC-EPS in a situation that a simplified version of the *breeding of growing modes* is used to generate the perturbed initial conditions instead of the EOF-method. For evaluations, a number of experiments are carried through, in which the configurations of the methods (region used to compute the unstable modes, perturbed fields, methodology to select the most unstable mode and perturbation method) are modified. Each experiment is evaluated in an operational suite during a one month period (January 2005) and in a case study. For the case study, the

first documented hurricane over the South Atlantic that occurred in March 2004 is considered as basic state. The aim is assessing the experiments in an episode of severe event that, in general, is a situation of low predictability.

The data and relevant descriptions about the methodology used to configure and execute the experiments as well as the statistical indexes computed to evaluate the results are presented in section 2. The results are discussed in section 3 and conclusions are presented in section 4.

2. Data and methodology

2.1 Initial conditions, climatology and period of evaluation

The control initial conditions (without perturbations) used in this study are the 1200 UTC daily spectral analyses obtained from NCEP by CPTEC/INPE to produce operational ensemble weather forecasting. The horizontal resolution of these analyses in the phase space is T126, i.e., triangular truncation in the wave number 126 which corresponds to approximately 0.975° longitude x latitude in the grid space. In the vertical, the atmosphere is discretized in 28 vertical sigma layers (L28). For subjective evaluations and to compute statistical indexes, these initial conditions are considered as the best estimate of the real state of the atmosphere.

The number of members and the range of each CPTEC-EPS simulation in this paper are the same used operationally at CPTEC/INPE. For each run, seven EOF or breeding based perturbations are generated and added (subtracted) to (from) the control initial condition creating a set of fourteen perturbed initial conditions. Each ensemble member represents an integration of the CPTEC-AGCM up to 15 days lead time from a perturbed initial condition or the control analysis. At the end of each EPS simulation an ensemble with 15 members is generated for each forecast range.

The period considered for evaluating the experiments in an operational suite is 1 to 31 January 2005 which corresponds to a period of summer season on the Southern Hemisphere. In South America, the January climatology indicates

intense convective activity over the north and center of the continent. The Intertropical Convergence Zone (ITCZ), the South Atlantic Convergence Zone (SACZ), the Subtropical Jet Stream, the Bolivian High and the Northeastern Brazilian Trough are the most significant synoptic scale systems that influence the weather conditions in this region in January. This period was chosen because of the relatively low predictability that numerical models exhibit over South America in this period (summer) in consequence of the strong influence that physical processes, especially deep convection, play in the forecasts over this region. We are particularly interested on the impact that modifications in the initial perturbations proposed in each experiment has in the quality of the ensemble forecast, especially over South America, in this period.

For the case study, analyses of each 12-hours from the period of Hurricane Catarina occurrence are considered, between 0000 UTC 20 March 2004 and 1200 UTC 28 March 2004.

The NCEP Reanalysis 2 climatology (Kanamitsu et al., 2002) is used to calculate analyses and ensemble forecasts anomalies and the climatological standard deviation of the 500-hPa geopotential height and 850-hPa wind fields.

2.2 CPTEC/INPE atmospheric general circulation model

The model used in this study is the CPTEC-AGCM at the same resolution of the analyses (T126L28) and with outputs in Gaussian-grid. Briefly, the CPTEC-AGCM is based on the spectral solution of the primitive dynamic equations, in the form of divergence and vorticity, virtual temperature, specific humidity and logarithm of the surface pressure, and inclusion of the sub-grid processes through parameterizations. Details of the model can be obtained in Kinter et al. (1997).

The main physical processes included in the CPTEC-AGCM are:

- Kuo-type deep convection;
- shallow convection;
- large-scale condensation;
- simplified biological model over continents (sSIB);

- bulk aerodynamics scheme over oceans;
- planetary boundary layer based on the Mellor-Yamada closure scheme;
- radiative fluxes (short wave and long wave) based on a band model;
- interaction of radiation with clouds.

2.3 The CPTEC/INPE operational EOF-based perturbation method

The perturbed initial conditions of the operational CPTEC-EPS are generated using the method developed by ZK1999 and applied firstly for hurricane forecasts with the Florida State University (FSU) AGCM. The method, called *EOF-based perturbation*, was developed based on the fact that during the first few days of the model integration the perturbation grows linearly. The procedures to generate perturbed analyses consists of:

- a) add small random perturbations to control analysis;
- b) integrate the model for 36 h (optimization time) starting from the control and from the perturbed initial conditions, saving results every 3 hours;
- c) construct the time series of difference field forecasts by subtracting the control forecasts from the perturbed forecasts at corresponding times;
- d) perform an EOF analysis for the time series of the difference fields over selected regions in order to obtain the fastest growing perturbations (considered as the eigenmodes associated to the largest eigenvalues). These modes are called *optimal perturbations*. More details of the EOF computation can be found in ZK1999;
- e) rescale the *optimal perturbations* to an established amplitude;
- f) generate an ensemble of initial conditions by adding (subtracting) these rescaled *optimal perturbations* to (from) the control analysis.

For hurricane forecasting, ZK1999 proposed perturbations in the hurricane initial position and the computation of the empirical orthogonal functions in the neighborhood of the hurricane. For global weather forecasting, Coutinho (1999) did not apply any perturbations in the initial position of any meteorological

systems. He also found that preliminary attempts to limit the perturbations in latitude and longitude, e.g., in a region over South America, were not satisfactory since that constraint had eliminated perturbation growth in regions that exert significant influence on the development of the synoptic systems. Better results were found using an extended region (45S-30N; 00E 360E). Another modification is associated to the amplitude of both random initial perturbations and optimal perturbations. ZK1999 considered that it was reasonable to assume that the perturbations had an order of magnitude comparable to that of 3-hour forecast (3 m/s for the wind field and 0.6 K for the temperature field). Coutinho (1999) obtained better results using the amplitudes 1.5 m/s and 0.7 K for the random initial perturbations and 5.0 m/s and 1.5 K (from Daley and Mayer, 1986) in the rescale procedure. These latter random initial perturbations and optimal perturbation amplitudes were adopted in the version of EOF-method implemented operationally at the CPTEC/INPE, and are also used in all experiments with EOF-method in this study.

2.4 Simplified version of breeding of growing modes

The simplified version of breeding method used in this study follows in general the guide lines presented in Toth and Kalnay (1993) and Toth and Kalnay (1997). However, some simplifications are adopted to make the method work properly for a large period of successive iterations with CPTEC-AGCM. With respect to the original version, two main modifications are implemented: the first one associated with the perturbed fields and the second one associated to the perturbation rescale. In the simplified breeding, instead of operating over vorticity and divergence fields, we have opted for calculating and rescale the perturbations using the zonal and meridional wind components. We adopted a rescale of perturbations according to a prior specified global standard deviation (horizontal and vertical) instead of a regional rescale like the one described in Toth and Kalnay (1997). The prior specified values of global standard deviation for each perturbed field are similar to those used at EOF-method for surface pressure and specific humidity fields, although slightly smaller values are used for temperature and wind

components. The perturbation magnitudes are: 1.0 hPa for surface pressure (from Anderson et al., 2005); 0.7 K for temperature; 1.5 m/s for zonal and meridional wind components. For specific humidity, the global rescale is performed at each vertical layer separately, using as reference the vertical background standard deviation distribution values presented in Derber and Bouttier (1999) for ECMWF global data assimilation system. Those values were linearly interpolated from ECMWF-AGCM vertical coordinates for CPTEC-AGCM sigma levels before their use. These interpolated values for each CPTEC-AGCM sigma levels are shown in Table 1.

Perturbation magnitudes equal to those used at EOF-method were tried for rescaling temperature and wind fields at *simplified breeding method*, but the perturbations became unstable (too large) after a few days of iteration of the method, so we adopted the values cited above, which were obtained from ZK1999.

Another aspect that should be mentioned is the fact that NCEP analyses, although of high quality, are not totally balanced with respect to CPTEC-AGCM. This can increase forecast errors, especially for shorter forecast ranges.

2.5 Experiments design

The main aspects considered to configure the procedure for generating perturbed initial conditions at each experiment are: the application of EOF-method to generate perturbations in midlatitudes; perturbations on surface pressure and specific humidity fields which are prognostic fields of the CPTEC-AGCM and are not perturbed in the operational version of CPTEC-EPS; and the replacement of the EOF-method by the simplified breeding of growing modes.

The application of EOF-perturbations in the surface pressure field may perhaps substitute partially the perturbations in the position of meteorological systems, originally used by ZK1999 in hurricane initial positions. For experiments with EOF-perturbations, the magnitude of random initial perturbations and in the rescale for surface pressure field is specified in 1.0 hPa. For specific humidity, the

initial random perturbations and the rescale are performed at each vertical model layer separately. The perturbation magnitudes are also those presented in Table 1.

While the perturbation growth over midlatitudes is mainly caused by dynamic instability (according to linear perturbation theory), in the tropics, the perturbations are strongly influenced by physical processes in smaller scales than those solved by models and exhibits a growth rate much smaller than that over the extratropics (Zhang, 1997; Reynolds et al., 1994). Therefore, it is more reasonable to generate perturbations over extratropics and tropics separately. Special treatment of perturbations over tropics was inserted at the ECMWF-EPS through the computation of tropical singular vectors over target areas (Barkmeijer et al., 2001; Puri et al., 2001). At NCEP, there is not a specific treatment for tropical perturbations, however the regional rescaling, based on analyses uncertainties, used operationally, contributes to enhance the ensemble mean skill over tropics and Southern Hemisphere (Toth and Kalnay, 1997). In those experiments which EOF-perturbations are applied in midlatitudes, we consider more suitable to calculate the perturbations for tropics and extratropics separately. By trying to get more adjusted EOF-perturbations for South America, regional perturbations are computed over two almost homogeneous different areas with respect to the influence of meteorological systems: a sector with tropical regime and strongly influenced by convective systems (Northern South America: 100W-10W; 20S-20N) and a region influenced by baroclinic systems (Southern South America: 110W-20W; 60S-20S). Overall, six regions are considered to compute EOF-perturbations depending on the configuration used for each experiment which will be described later:

- Northern Hemisphere (NH): 0-360W; 20N-90N;
- Southern Hemisphere (SH): 0-360W; 20S-90S;
- Tropics (TR): 0-360W; 20S-20N;
- Extended Tropics (ETR): 0-360W; 45S-30N;
- Northern South America (NSA): 100W-10W; 20S-20N;
- Southern South America (SSA): 110W-20W; 60S-20S.

For hurricane prediction, ZK1999 found that the eigenvector associated to the largest eigenvalue (first mode) was the mode whose coefficients present the largest growth rate with respect to time. Consequently, they used it as *optimal perturbation*. During this study, we verified that the coefficients of first mode do not always present the largest growth rate. We noted that the mode whose coefficients increase rapidly with time could be different for both each perturbed region (described earlier) and each perturbed analysis field. So, an experiment is proposed in which the methodology used to select the *optimal perturbation* is based on the linear time tendency exhibited by the coefficients of each mode. The mode whose coefficients show major growth rate in the optimization time (here specified in 36-hours) is selected.

In order to evaluate which modifications in the operational CPTEC-EPS perturbation scheme produce more significant impact on ensemble forecast quality, seven experiments are performed: experiment OPER, considered as a reference to other experiments, represents the operational configuration used currently at CPTEC/INPE, in this case, the zonal and meridional wind components (U,V) and temperature (T) fields are perturbed over an extended tropical region (TRE, 0-360E; 45S-30N); in the second experiment (EXT1), perturbations are computed for three global regions, Northern Hemisphere (NH, 0-360E; 20N-90N), Southern Hemisphere (SH, 0-360E; 90S-20S) and tropics (TR, 0-360E; 20S-20N) and the perturbed fields are again U, V and T; in experiment defined as TROP (third one) the perturbed region is the same of the operational version (OPER), but includes perturbations on surface pressure (P) and specific humidity (Q) fields which are not perturbed in the former experiment; in fourth experiment (EXT2), perturbations on three global regions NH, SH and TR are combined with additional perturbations on P and Q fields; in experiment ETSA (fifth one), besides perturbations in midlatitudes (NH and SH) and tropics (TR), additional perturbations for two different sectors of South America (Northern of South America - NSA, 100W-10W, 20S-20N and Southern South America - SSA, 110W-20W, 60S-20S) are computed, and the perturbed fields are P,T,Q,U and V; in sixth experiment (LNCR), the impact of selecting the unstable modes through the linear growth rate of EOF coefficients instead of always selecting the first mode as the most unstable is evaluated, in this experiment, perturbations are computed for all five perturbation regions NH, SH, TR, NSA

and SSA, and for P, T, Q, U and V analysis fields; the last experiment (BRCP) consists of using the *simplified breeding of growing modes* method to generate perturbed initial conditions with CPTEC-AGCM. A complete list of the experiments and their respective characteristics are presented in Table 2.

2.6 Forecast performance measures

In this study, the quality of atmospheric patterns prediction and probability forecasts are assessed through the evaluation of ensemble mean and probability distribution given by ensemble members, respectively. The perturbation growth during model integration is considered through the computation of the ensemble spread. In order to measure the quality of ensemble mean forecasts, the pattern anomaly correlation (PCA) and root mean square error (RMS) are calculated for the considered period. The ensemble spread is measured through the standard deviation of ensemble members with respect to ensemble mean. The quality of probabilistic forecast is verified by calculating the Brier Skill Score (BSS) and its components (reliability-Rel, resolution-Res and uncertainty) according to Wilks (1995) and Buizza et al. (2005). The 500-hPa geopotential height (Z500) field over Northern Hemisphere (NH, 20N-90N), Southern Hemisphere (SH, 90S-20S), Tropics (TR, 20S-20N), and South America (SA, 110W-10W; 60S-15N) is used in the evaluation. The Z500 field provides relevant information about of synoptic atmospheric pattern scale, mainly over midlatitudes. Over tropics, where the horizontal wind is more important than the geopotential height anomaly, the evaluation is also being computed to zonal and meridional wind components at 850-hPa (U850 and V850). The components of Brier Skill Score are computed using the probability forecasts of 500-hPa geopotential height anomaly greater or lesser than one climatological standard deviation. The U850 and V850 fields are considered separately and the probability forecast of U850 and V850 anomaly greater or lesser than 5 m/s is evaluated. The probability intervals are established according to the number of ensemble members, following the methodology presented on the report *Manual on the Global Data-Processing System*, edited by World Meteorological Organization (WMO, 1992).

The quality of ensemble perturbations is investigated using the methodology developed by Wei and Toth (2003), called *perturbation versus error correlation analysis* (PECA). This tool is very useful in comparing ensembles produced from distinct analyses, since it is not sensitive to the quality of the initial conditions. The PECA measures the amount of variance that individual and/or optimally combined ensemble perturbations can explain in forecast error fields. It is computed firstly for 500-hPa geopotential height in order to evaluate the synoptic pattern of perturbations, mainly over midlatitudes. In an attempt to investigate the ability of the ensemble perturbations to capture the three-dimensional forecast error structure, the PECA is also computed for three variables, temperature (T) and wind (U,V) at three levels, 850, 500 and 250 hPa. Following Wei and Toth (2003), a new variable p is defined $p=(U,V,\alpha T)$, where $\alpha=\sqrt{C_p/T_r}$, $C_p = 1004.0 \text{ J kg}^{-1} \text{ K}^{-1}$ is the specific heat at constant pressure for dry air and T_r is a reference temperature. For each pressure level, T_r is obtained by linear interpolation from *Standard Atmosphere Data* (Holton, 2004).

Each CPTEC-EPS run produces an ensemble of 15 forecasts (14 perturbed and 1 control) integrated for up to 15 days. To compute statistical indexes, except for PECA, the fields from both forecasts and analyses are interpolated to a regular grid with 2.5 x 2.5 degrees, according to WMO (1992). The results presented in figures represent the average of statistical indexes over the period considered, from 1 to 31 January 2005.

3. RESULTS

The presentation of the results is organized in two parts: the first one is about the assessment of experiments in an operational suite, on which the mean values of statistical indexes are presented; in the second part, the experiments are evaluated for the prediction of an intense cyclone that occurred in March 2004 over the South Atlantic, in this case, the analyzed aspects in each experiment are the predictions of the cyclone trajectory and the value of the cyclone central pressure.

3.1 Evaluation of experiments in an operational suite

In this section, the results of experiments are assessed through the average of the statistical indexes over January 2005, described in section 2.6. Aiming to investigate the impacts of the modifications in the initial perturbation procedure of each experiment on the performance of CPTEC-EPS, we compare the results of the control experiment (OPER) with the results of other experiments. Firstly, the impact of including perturbations on the surface pressure and humidity specific fields and the application of EOF-based perturbations in the extratropics is evaluated. Next, the impacts of applying regional perturbations over South America, the selection of optimal perturbations based on the growth of the EOF-coefficients time series and, finally, the experiment with the simplified breeding method are assessed. Special attention is given to the impacts of each experiment on the ensemble performance over South America Region.

a) Impact of computing additional EOF-perturbations for extratropics and for surface pressure and specific humidity fields

In terms of pattern anomaly correlation (Fig. 1) the ensemble mean forecasts present better performance than the control prediction. This result is more evident for lead times longer than five days when the 500-hPa geopotential height field over extratropics is evaluated, and for almost all lead times when the 850-hPa wind components over tropics is considered. We notice that there are just small differences amongst the performance of ensemble mean predictions of the experiments. For lead times longer than eight days, the experiment EXT2, in which extratropical EOF-perturbations were combined with perturbations on surface pressure and specific humidity fields, presents a slight advantage with respect to experiments OPER, TROP and EXT1, mainly for the NH region. Considering RMS and spread (Fig. 2), it is verified that the expansions of the perturbed region and the perturbed fields (experiments EXT1 and EXT2) cause reasonable increase of the ensemble spread over the NH. For 850-hPa horizontal wind components in the tropics, perturbations on surface pressure and on specific humidity (experiment TROP) increase the performance of the ensemble mean;

however, they diminish the ensemble spread. The expansion of the perturbation regions in experiment EXT1 has a small impact over ensemble mean skills for horizontal wind field over the tropics. The results of experiment EXT2, over the tropics, are similar to that from TROP. This suggests that perturbations on P and Q fields are more relevant than perturbations over the midlatitudes to the performance of the ensemble mean over the tropics.

The Brier Skill Score index is positively oriented, so the higher BSS values indicate better probability predictions. The same consideration is true for the BSS resolution component (Res), which summarizes the ability of the forecasts to discern subsample forecast periods with different relative frequencies of the event. On the other hand, the BSS reliability component (Rel), which measures the calibration or conditional bias of the forecasts, is negatively oriented. The evaluation of the probability forecasts, according to BSS index (Fig. 3) and its components (Fig. 4), indicates that the expansion of the perturbed regions (experiment EXT1) contributes to improve the probability forecast over the NH. However, this modification does not cause significant impact over any other regions. The application of perturbations on P and Q fields in experiment TROP produces positive impacts on the performance of probability forecasts, especially over the regions TR and SA. However, is the combination of expansion of the perturbed regions and perturbations on P and Q fields (experiment EXT2) which presents the best results according to BSS and BSS components. Fig. 4 also shows that the configuration in the initial perturbation procedure of each experiment impacts on each assessed field differently. It can be verified improvements on the forecast resolution as well as on the forecast reliability for Z500 anomalies, while more significant impacts are observed on the forecast reliability for anomalies of 850-hPa wind components. The results indicate that for U850 and V850 anomalies over tropics (Fig. 4e-f), the inclusion of perturbations on P and Q fields in experiment TROP has a greater contribution in the improvement of the ensemble forecast reliability than the extratropical perturbations of EXT1. These results indicate that the slight increase of the BSS for wind over the tropical region (Fig. 3e-f), mainly for experiments TROP and EXT2, is associated to a decrease in the forecast probability bias when perturbations over the extratropics combined with perturbations on P and Q fields are applied.

The quality of the perturbations for each experiment is measured by the PECA index. While the ensemble spread can be easily changed by multiplying the initial perturbations by a scalar number, perfect pattern spread is not affected by such a change. The pattern spread can only be changed through the introduction of more diversity in the initial ensemble perturbation patterns. The PECA measures the amount of variance that individual and/or optimally combined ensemble perturbations can explain in forecast error fields. As higher the PECA values are, the better the ensemble is able to capture the forecast errors (Wei and Toth, 2003). In this study, an average over 14 individual PECA values, i.e., 14 correlations between the forecast errors and 14 individual ensemble perturbations (indicated by the acronym *sin*), and the PECA values for a correlation between the forecast errors and an optimal combination of the 14 individual ensemble perturbations (indicated by the acronym *opt*) are presented, for each forecast lead time. For 500-hPa geopotential height field (Fig. 5) over NH, the inclusion of perturbations on extratropics (experiment EXT1) produces an increase in the amount of forecast error variance explained by the ensemble perturbations in both individually and optimally combined cases. Additional perturbations on P and Q fields in experiment EXT2 show results similar to that from experiment EXT1 over the NH. Over the SH, the introduction of extratropic perturbations in experiment EXT1 is the configuration that presents higher PECA values, especially for individual perturbations. Over tropics, the operational configuration (experiment OPER) presents better results in the two first prediction days. Beyond the third day, the variance of forecast errors is better explained by the perturbations of experiment EXT2. Over the SA, the amount of variance of forecast errors explained by individual perturbations is closely the same in all experiments. However, the optimal combination of perturbations shows that it is the operational configuration (experiment OPER) that presents higher PECA values for up to 8 days. At longer lead times the PECA values for all experiments become very similar. The PECA values calculated using the three-dimensional structure of the forecast errors and of the ensemble perturbations, which involve the fields U, V and T at 850, 500 and 250 hPa levels, are shown in Fig. 6. It is observed that the application of extratropical EOF-perturbations in experiment EXT1 and their combination with perturbations on P and Q fields in experiment EXT2 present higher PECA values than those from OPER and TROP. This suggests that the

computation of extratropical EOF-perturbations could improve the quality of the CPTEC/INPE ensemble perturbations with respect to the operational configuration (experiment OPER).

b) Impact of regional perturbations computed over SA

In this section, the impact of including regional perturbations over the South America is assessed. In experiment ETSA, besides the extension of initial perturbations for extratropics, and the inclusion of perturbations on P and Q fields, two South America sub-regions are considered in order to compute regional perturbations: Northern South America (NSA: 100W-10W; 20S-20N) and Southern South America (SSA: 110W-20W; 60S-20S). The results of this experiment are presented in Figs. 7-12. It is observed that, for hemispheric domains (NH, SH and TR), the pattern anomaly correlations, RMS and forecast spread values are similar to those of experiment EXT2, in which there is not specific perturbations over South America. However, looking at the statistical indexes for the South America region, positive impacts can be noticed by the inclusion of such perturbations. Table 3 presents the difference between the statistical indexes of experiments ETSA and EXT2, computed for Z500 over the SA region. An increase in the pattern anomaly correlation and in the forecast spread, as well as, a decrease in the RMS, in almost all forecast lead times are verified. For probability forecasts over SA is observed that, except for the first forecast day, the statistical indexes indicate positive impacts of the regional perturbations. The PECA indicate a slight increase of forecast errors variance explained by ensemble perturbations, except in some few forecast lead times.

c) Selection of the optimal perturbations based on the linear growth rate of EOF coefficients

In this section, the impact of selecting the most unstable mode, based on the linear tendency exhibited by the EOF coefficients according to the slope of a straight line fit to such coefficients using the least square method, is assessed. This

experiment is called LNGR. At the operational configuration and at other experiments of this study, the mode associated to the largest eigenvalue is selected as the most unstable. ZK1999 found that the eigenvector corresponding to the largest eigenvalue was the mode whose coefficients presented larger growth tendency with respect to time. However, the perturbations of their experiments were confined to the neighborhood of hurricanes. The motivation for performing this experiment came up after verifying that in some situations, depending on the perturbed region and on the perturbed field, the EOF coefficients of the first mode did not exhibit growth with time. On the contrary, they presented a negative growth tendency. The configuration of the initial perturbations of experiment LNGR, i.e., perturbed regions and perturbed fields are the same of experiment ETSA. The latter experiment is used as reference to assess the impact of applying this new methodology to select the optimal perturbations.

According to the methodology for computing the EOF modes, presented in the section 2.3, for each random perturbation, added to the control analysis at the first part of the procedure to compute optimal perturbations, 11 modes (eigenvectors) are obtained. Their coefficients are examined aiming to find out which one presents the largest growth tendency. These 11 modes are ordered according to the magnitude of the corresponding eigenvalue ($\lambda_{i=1,\dots,11}$), such that $\lambda_1 > \lambda_2 \dots > \lambda_{11}$. As mentioned earlier, for the regions used for computing the perturbations, the coefficients of the first mode do not always show the largest growth rate. Considering the period (31 days) and the 5 regions used in experiment LNGR, the frequency at which the first 4 modes were selected as *optimal perturbation* is presented in the Fig. 13, for each perturbed field. The first 4 modes are selected in more than 95% of the cases, except for surface pressure in which they are selected around 88% of the cases (figures not included). It is clearly noticed that mode 2 is the most frequently selected for perturbations on P, T and Q fields. However, for wind field mode 1 is most frequently selected and represents individually around 70% of the selected modes. The second most selected is mode 2, which is selected around 25% of the cases. On the tropical region, at least for the considered period, the first mode of wind field was selected in all runs (Fig. not shown). This result agrees with that of ZK1999 who found larger growth rate for the coefficients of the first mode. However, when the perturbations for the temperature field are analyzed, the results indicate that the second mode is predominantly selected. This

result differs from results of ZK1999, who obtained a larger growth rate for the first mode. This disagreement may be associated to the different regions used for computing the perturbations and the perturbations on surface pressure and specific humidity fields that were not applied on their study. This result will be better investigated in a future work.

The average statistical indexes of experiment LNGR are shown in Figs. 7-12. A general analysis indicates that the selection of the optimal perturbations by the linear growth of the EOF coefficients has a slightly positive impact on the ensemble performance over the extratropics (NH and SH) while over the tropics the impact is slightly negative. For SA, the difference between the indexes of experiments LNGR and ETSA (Table 4) suggests that the methodology used in experiment LNGR to select the most unstable modes is slightly better than always selecting the first mode, as used in experiment ETSA. This result becomes more evident when the indexes assessed are pattern anomaly correlations, RMS and PECA. For other indexes, there is not a well-defined indication of improvement.

d) Impact of perturbations based on simplified breeding of growing modes

The experiment on which the simplified breeding method is used to produce perturbed initial conditions is called BRCP. In this experiment we attempt to identify if using the scheme adopted at CPTEC/INPE for operational ensemble weather predictions, in which the control analyses are not produced with the same model (they are produced at NCEP), the breeding method can produce satisfactory perturbations for CPTEC-EPS. Moreover, we take the results with simplified breeding as a reference in an attempt to identify problems and/or deficiencies of EOF-method, used currently for operational ensemble forecasts at CPTEC/INPE. The results of experiment BRCP are compared to the results of experiment ETSA since it presented slightly better results than the operational one. It should be kept in mind during the evaluation of results that, even though the methodology used for generating the perturbations is similar to that used at NCEP, the simplified version used here has significant differences. The most important ones are: the model used for obtaining the perturbations is not the same used to generate the analyses. This can allow the presence of systematic errors of the NCEP model on

the perturbations; the rescale of the perturbations is performed according to a global metric, instead of the regional rescale used at NCEP. The regional rescale is recognized as more adequate and could produce better perturbations.

The results of experiment BRCP are also presented in Figs. 7-12. It can be observed that, despite using a simplified version, the perturbations of breeding method produce ensemble predictions competitive to those of the EOF-method. Looking at the performance of ensemble mean, it is observed that the pattern anomaly correlation and the RMS are very similar to those of experiment ETSA, over NH. Over the Southern Hemisphere, the Tropics and South America, the pattern anomaly correlations are slightly smaller and the RMS, slightly worse. An interesting result of experiment BRCP is the increase of the ensemble spread for all regions in almost forecast lead time, except for the two first prediction days. Improvements on probability forecasts are verified over NH, while in the other regions is seen a slight decrease in the forecast quality. In terms of PECA, the forecast perturbations of experiment BRCP explain the variance of forecast errors better than those of other experiments over the NH and the SH, when Z500 field is assessed. When the three-dimensional and multivariable structure (Fig. 12) is analyzed, larger values of PECA for experiment BRCP are observed in all regions for predictions longer than 3 days over the extratropics, 7 days over the tropics and 5 days over the SA, when individual perturbations are considered. The breeding-ensemble forecasts are comparatively more benefited by optimal combination of the forecast perturbations leading to an anticipation of the range on which they better explain the variance of forecast errors, for 2 days over the extratropics, 5 days over tropics and 4 days over SA.

The slightly inferior performance of the simplified breeding method over regions SH and TR may be associated to the lack of regional rescale as in the original version. According to Toth and Kalnay (1997) that procedure presents more significant improvements on the performance of NCEP ensemble forecasts exactly over those two regions.

3.2 Case study: cyclone Catarina (March 2004)

Besides the evaluations of the experiments in an operational suite presented in the previous sections, a case study about the prediction of a severe event is carried out. The aim is to understand better the influence that the modifications in the procedure of producing perturbed analyses, suggested in this study, has on the performance of the CPTEC-EPS. In general, severe events are difficult to be predicted by numerical models, especially in the low resolution (about 100 Km) used here. However we try to assess if such modifications aggregate useful information to CPTEC/INPE ensemble weather forecasts.

The selected meteorological event, called Catarina occurred in March 2004 near the Brazilian coast. It was characterized in its mature phase by an eye (Fig. 14), typical of intense tropical systems such as hurricanes, strong winds in its board and westward displacement. More detailed analyses indicate that Catarina initiated as an extratropical cyclone embedded in a frontal system and underwent a tropical transition two days later under low vertical wind shear over near-average sea surface temperatures (Pezza and Simmonds, 2005). Satellite estimates indicated that the cyclone central pressure was about 970-975 hPa, and sustained winds of up to 35 m/s (Silva Dias et al., 2004).

Figure 15 shows the representation of Catarina by CPTEC-MCGA initial condition at 1200 UTC 24 March 2004 as seen by sea mean level pressure and wind intensity fields, in the horizontal resolution used in this study. It can be verified that the analysis significantly overestimates the cyclone central pressure (underestimates its intensity). For this situation, the value of the analysed pressure inside the center of the system is around 1008 hPa. The wind magnitude on the cyclone boundaries is relatively smaller than those estimated by satellite. According to the analysis, the largest wind speed occurs at the southern part of the system with intensity around of 14 m/s. The underestimation of the cyclone intensity by the analysis may be associated to the relatively low resolution used in this study and/or due to the lack of conventional observations in this region. The inadequate representation of the system by the initial condition makes the simulation of the event by the numerical models difficult. Zhu and Thorpe (2006) found that an accurate representation of extratropical cyclones by initial conditions is essential to be able to predict the development of these systems with some skill.

The trajectory of Catarina, as represented by the NCEP analyses, is given in Fig. 16. The space between two points represents the displacement of the system in a period of 12 hours. The initial point of the trajectory (northern-most point) indicates the position of the system at 1200 UTC 20 March 2004. The last point, when the system had already reached the continent, was 1200 UTC 28 March 2004. Initially, the system displaced southeastward. Then, after a change in its dynamic structure from extratropical cyclone into tropical cyclone, it turned westward, moving to the continent. Despite the low resolution of the analyses used in this study, the trajectory shown in Fig. 16 is similar to that obtained from ECMWF high resolution analyses by Pezza and Simmonds (2005).

This case study aims to assess mainly the ensemble prediction of the cyclone trajectory and the value of the central pressure after the tropical transition of the cyclone. Moreover, the impact of the modifications implemented in experiments described in the previous sections on the performance of the CPTEC-EPS is evaluated. The information about the trajectory and intensity of the cyclone are valuable for an analysis of striking risk and damage of the system.

The prediction of Catarina begins at 1200 UTC 24 March 2004. In Fig. 17a, it is clearly noticed that the model presents a deficiency in simulating the evolution of the system. The control prediction (dashed lines) is able to simulate the system only up to forecast hour 48. From 1200 UTC 24 March until 0000 UTC 26 March, Catarina moved northwest, then, it turned westwards. The cyclone trajectory predicted by the control forecast is a more northward displacement than the observed one. The ensemble members (dots) of the operational configuration (experiment OPER) present large spread in the forecast of the cyclone position. Some members are able to simulate the system up to forecast hour 72, and the change in the system displacement direction. However, in general, the ensemble members also indicate trajectories more northern than the observed one. The results of other experiments (Figs. 17b-g) indicate that extratropic perturbations and perturbations on P and Q fields contribute to increase the spread of the trajectories predicted by the ensemble members. Overall, experiments EXT2 and ETSA present better results. The inclusion of perturbations on surface pressure and specific humidity fields (experiments TROP, EXT2, ETSA and LNCR) cause an increased dispersion of the cyclone initial position when compared to the experiments without those perturbations (experiments OPER and EXT1). This

result suggests that those perturbations, mainly on the surface pressure, can produce an effect similar to that applied in the cyclone position by Zhang (1997).

Figure 18 shows the results of central pressure predictions. It is noticed that the cyclone central pressure value is overestimated by the control prediction (dashed line). This result was also obtained by Bonatti et al. (2006) in a simulation of Catarina episode using a high resolution (T511L64, about 22 Km) version of CPTEC-AGCM model. The overestimate of the cyclone central pressure is due in part to the position where the model locates the maximum heating source (500-hPa) when it was observed at 850-hPa in the analyses (figures not included).

For experiment OPER (Fig. 18a), it is verified that forecasted values (dots) are larger than those observed at all forecast lead times. Although the ensemble mean (dotted line) has been able to indicate the cyclone for 12 hours beyond that of the control forecast, it indicates values very close to that of the control prediction. The application of perturbations on the extratropics in experiment EXT1 (Fig. 18c) produces a small growth on the ensemble spread and improves slightly the ensemble mean prediction. However, the predicted pressure values are higher than those observed. With additional perturbations on surface pressure and specific humidity fields in experiment TROP (Fig. 18b), the ensemble mean indicates the cyclone up to forecast hour 72, although the ensemble mean values are still very close to the control values at the first few forecast lead times. The inclusion of additional perturbations on the extratropics and on P and Q fields in experiment EXT2 increases the spread of the ensemble members and becomes the central pressure forecast of the ensemble mean closer than the analyses values. Still, only in the forecast hour 12, the ensemble members capture the value verified in the analysis. The impact of regional perturbations over South America on the performance of ensemble forecasts can be assessed through the results of experiment ETSA (Fig. 18e). It is evident that such perturbations contribute to produce forecast values of central pressure lower than those obtained from the control forecast. The ensemble mean values are relatively closer to the observed values. The results of experiment LNGR (Fig. 18f) are similar to those of experiment ETSA, except that a decrease in the ensemble spread is observed. The results from experiments ETSA and LNGR suggest that most improvements on the forecast performances, with respect to other experiments, are associated to the application of regional perturbations over South America. This result is in

agreement with those of ZK1999 and Puri et al. (2001) who suggest the computation of additional perturbations over a limited area on the neighborhood of tropical cyclones in order to improve the forecasts of severe meteorological systems. Experiment BRCP presents similar results to the operational version, although a small increase on the ensemble spread is verified. Part of the low impact of simplified breeding method in the ensemble forecasts for Catarina episode must be associated with the global rescale used in this study. It is possible that regional perturbations near Catarina region have been smoothed by the global rescale and a regional rescale would probably produce better results.

4. Discussion and conclusions

The quality of numerical weather prediction has improved significantly in recent decades. Some factors that have contributed largely to this are: rapid computational development, advent of satellite data assimilation and better representation of atmospheric phenomena by numerical models. In this context, the ensemble weather forecasting were developed as a natural consequence of the knowledge of atmosphere chaotic behavior, the impossibility of eliminating all initial conditions uncertainties and the incomplete representation of physical and dynamical atmosphere processes within numerical models. The meteorological centers ECMWF and NCEP were pioneers in implementing operational ensemble weather forecasting. By using different methods to generate perturbed initial conditions they started their EPS systems in 1992. Later on, other centers implemented their own EPS systems. They adopted one of those methods to produce perturbed analyses to run their models or apply new methodologies, such as implemented at Meteorological Service of Canada (MSC) and at CPTEC/INPE. Trying to produce suitable forecasts over tropical region, CPTEC/INPE adopted the EOF-method which was initially developed to generate ensemble forecasts for tropical systems. In this study, we evaluate the CPTEC-EPS using statistical indexes in an attempt to identify forecast deficiencies and suggest alternatives to solve or reduce them by modifying some configurations of the operational EOF-method used to generate perturbed initial conditions. One of the most important issues addressed here is the impact of EOF perturbations computed over the

extratropics on the quality of CPTEC-EPS forecasts. Under perfect model hypothesis, seven experiments were performed by modifying the regions used to compute the initial perturbations, extending the perturbations to analyses fields that were not perturbed yet (surface pressure and specific humidity) and implementing a simplified version of breeding-method to CPTEC-AGCM. All experiments were evaluated in an operational suite and for a case study of a severe event.

We found that both the extension of EOF-perturbations towards the extratropics and additional perturbations in P and Q fields have a positive impact over CPTEC-EPS performance, mainly over NH. Results indicate clearly that more improvements can be achieved by combining these two modifications in the perturbed analyses generation procedure. Over South America, for those experiments in which regional perturbations are combined with hemispheric perturbations (ETSA and LNGR), forecasts perform better than those where only global perturbations are applied. The simplified breeding-method added positive aspects for CPTEC-EPS performance, such as smaller ensemble mean RMS and larger ensemble spread.

The results from the case study reveal that the cyclone intensity is underestimated by initial conditions, i.e., the minimum central pressure is higher and the wind on the cyclone periphery is weaker than those estimated from satellite information. For operational ensemble run (experiment OPER) started at 1200 UTC 24 March 2004, the forecasts overestimate the analyses pressure values and do not indicate a well configured cyclone after a 48-hours forecast lead time. Additional perturbations in the extratropics and in P and Q fields extend that range for an extra 12-hours, it also improves forecasts of cyclone central pressure. However, the cyclone track was captured only by few members. The best results were obtained with experiment in which additional regional perturbations over South America are computed (experiments ETSA and LNGR).

In general, the application of EOF-method to perturb midlatitudes and additional perturbations for surface pressure and specific humidity fields, as well as the use of simplified breeding-method produce positive impacts on the quality of CPTEC-EPS. However, in none of the experiments the under-dispersion of the system was totally solved. We suppose that part of the problem is associated to rapid error growth of CPTEC-AGCM in the first few days of integration model.

Therefore we intend to investigate, in a future work, the influence of perturbations in physical and dynamical processes of CPTEC-AGCM in the quality of CPTEC/INPE ensemble forecasts, as has been done operationally at MSC and ECMWF. Moreover, another point that will be investigated is the use of a control initial condition created by CPTEC-AGCM itself to generate the perturbed initial conditions. Currently, a data assimilation cycle based on Physical-space Statistical Analysis System (Cohn et al. 1998) associated with CPTEC-AGCM is running in a pre-operational suite. The implementation of a Local Ensemble Kalman-Filter (Ott et al., 2004) version for data assimilating and ensemble forecasting is in progress at CPTEC/INPE and could also be evaluated.

The results from the experiments with additional perturbations on the extratropics and on P and Q fields, as well as, regional perturbations over South America encourage an operational implementation of these modifications at CPTEC-EPS in order to diminish the ensemble system deficiencies and improve the quality of CPTEC/INPE ensemble forecasts.

Acknowledgements

We thank Dr T. N. Krishnamurti and Dr. Z. Zhang from the Florida State University (FSU - USA) for providing the original computational procedures of EOF-method. We would also like to thank Dr. M. M. Coutinho for your effort to adapt the original procedures of EOF-method for CPTEC-AGCM and your helpful support during the operational implementation of the CPTEC-EPS.

References

- Anderson JL, Wyman B, Zhang S, Hoar T (2005) Assimilation of Surface Pressure Observations Using an Ensemble Filter in an Idealized Global Atmospheric Prediction System. *J Atmos Sci* 62: 2925-2938
- Åtger F (1999) The skill of ensemble prediction systems. *Mon Wea Rev* 127: 1941-1953
- Barkmeijer J, Buizza R, Palmer TN, Puri K, Mahfouf J-F (2001) Tropical singular vectors computed with linearized diabatic physics. *Q J R Meteorol Soc* 127: 685-708
- Bishop CH, Etherton BJ, Majumdar S (2001) Adaptive sampling with the ensemble transform Kalman filter. Part I: theoretical aspects. *Mon Wea Rev* 129: 420-436
- Bonatti JP, Rao VB, Silva Dias PL (2006) On the westward propagation of Catarina storm. *Proceedings of 8th International Conference on Southern*

Hemisphere Meteorology and Oceanography, 24-28 April 2006, Foz do Iguaçu, Pr, Brazil

- Buizza R, Houtekamer PL, Toth Z, Pellerin G, Wei M, Zhu Y (2005) A comparison of the ECMWF, MSC, and NCEP Global Ensemble Prediction Systems. *Mon Wea Rev* 133: 1076-1097
- Buizza R, Miller MJ, Palmer TN (1999) Stochastic simulation of model uncertainties in the ECMWF ensemble prediction system. *Q J R Meteorol Soc* 125: 2887-2908
- Buizza R (1997) Potential forecast skill of ensemble prediction and spread and skill distributions of the ECMWF ensemble prediction system. *Mon Wea Rev* 125: 99-119
- Cohn SE, Da Silva A, Guo J, Sienkiewicz M, Lamich D (1998) Assessing the Effects of Data Selection with the DAO Physical-space Statistical Analysis System. *Mon Wea Rev* 126: 2913-2926
- Coutinho MM (1999) Previsão por conjuntos utilizando perturbações baseadas em componentes principais. (Ensemble prediction using principal-component-based perturbations). M. S. Dissertation, INPE, S. J. Campos, SP, Brazil, 136 pp
- Daley R, Mayer T (1986) Estimates of global analysis error from the global weather experiment observational network. *Mon Wea Rev* 114: 1642-1653
- Derber J, Bouttier F (1999) A reformulation of the background error covariance in the ECMWF global data assimilation system. *Tellus* 51A: 195-221
- Farina L, Mendonça AM, Bonatti JP (2005) Approximation of ensemble members in ocean wave prediction. *Tellus* 57A: 204-216
- Hamill TM (2002) Ensemble-based data assimilation. Seminar Proceedings on Predictability of weather and climate, 9-13 September 2002, ECMWF, Reading, UK
- Holton JR (2004) *An Introduction to Dynamic Meteorology*. 4th ed., Elsevier Academic Press, 535 pp
- Hoskins BJ, Karoly J (1981) The steady linear response of a spherical atmosphere to thermal and orographic forcing. *J Atmos Sci* 38: 1179-1196
- Houtekamer PL, Lefaiivrem L, Derome J, Ritchie H, Mitchell HL (1996) A system simulation approach to ensemble prediction. *Mon Wea Rev* 124: 1225-1242
- Kalnay E, Corazza M, Yang S-C, Hunt B, Kostelich E, Ott E, Patil DJ, Szunyough I, Yorke J, Zimin A (2002) Data assimilation via local ensemble Kalman filtering. Seminar Proceedings on Predictability of weather and climate, 9-13 September 2002, ECMWF, Reading, UK
- Kanamitsu M, Ebisuzaki W, Woollen J, Yang S-K, Hnilo JJ, Fiorino M, Potter GL (2002) NCEP-DEO AMIP-II Reanalysis (R-2). *Bull Amer Meteor Soc* 83: 1631-1643
- Kinter JL, DeWitt D, Dirmeyer PA, Fennessy MJ, Kirtman BP, Marx L, Schneider EK, Shukla J, Straus DM (1997) The COLA atmosphere-biosphere general circulation model Volume 1: Formulation. Center for Ocean-Land-Atmosphere Studies. Calverton, MD, COLA Staff, Report N.o 51

- Krishnamurti TN, Kishtawal CM, Zhang Z, LaRow T, Bachiochi D, Williford E (2000) Multimodel ensemble forecasts for weather and seasonal climate. *J Climate* 13: 4196-4216
- Liebmann B, Hartmann DL (1984) An observational study of tropical-midlatitude interaction on intraseasonal time scales during winter. *J Atmos Sci* 41: 3333-3350
- Lorenz EN (1963) Deterministic non-periodic flow. *J Atmos Sci* 20: 130-141
- Lorenz EN (1965) A study of the predictability of a 28-variable atmospheric model. *Tellus* 17A: 321-333
- Lorenz EN (1969) The predictability of a flow which possesses many scales of motion. *Tellus* 21A: 289-307
- Mendonça AM, Bonatti JP (2006) Experiments with EOF-based perturbation method to ensemble weather forecasting in midlatitudes. Proceedings of 8th International Conference on Southern Hemisphere Meteorology and Oceanography, 24-28 April 2006, Foz do Iguaçu, Pr, Brazil
- Mo KC, Higgins RW (1998) The Pacific-South American Modes and Tropical Convection during the Southern Hemisphere Winter. *Mon Wea Rev* 126: 1581-1596
- Molteni F, Buizza R, Palmer TN, Petroliagis T (1996) The ECMWF ensemble prediction system: Methodology and validation. *Quart J Roy Meteor Soc* 122: 73-119
- Ott E, Hunt BR, Szunyough I, Zimin AV, Kostelich EJ, Corazza M, Kalnay E, Patil DJ, Yourke JA (2004) A local ensemble Kalman filter for atmospheric data assimilation. *Tellus* 56A: 415-428
- Palmer TN (1988) Large-scale tropical, extratropical interactions on time-scales of a few days to a season. *Aust Met Mag* 36: 107-125
- Pezza AB, Simmonds I (2005) The first South Atlantic hurricane: Unprecedented blocking, low shear and climate change. *Geophys Res Lett* 32: L15712, doi:10.1029/2005GL023390
- Puri K, Barkmeijer J, Palmer TN (2001) Ensemble Prediction of tropical cyclones using targeted diabatic singular vectors. *Q J R Meteorol Soc* 127: 709-731
- Rabier F, Järvinen H, Klinker E, Mahfouf J-F, Simmons A (2000) The ECMWF operational implementation of four-dimensional variational assimilation. I: experimental results with simplified physics. *Quart J Roy Meteor Soc* 126: 1143-1170
- Reynolds CA, Webster PJ, Kalnay E (1994) Random error growth in NMC's global forecasts. *Mon Wea Rev* 122: 1281-1305
- Silva Dias PL, Silva Dias MAF, Seluchi M, Diniz FA (2004) O ciclone Catarina: Análise preliminar da estrutura, dinâmica e previsibilidade (in Portuguese). XIII Brazilian Meteorological Conference, Braz Meteorol Soc, 29 August-3 September 2004, Fortaleza, CE, Brazil
- Simmons AJ (1982) The forcing of stationary wave motion by tropical diabatic heating. *Quart J Roy Meteor Soc* 108: 503-534

- Toth Z, Kalnay E (1997) Ensemble forecasting at NCEP and the breeding method. *Mon Wea Rev* 125: 3297-3319
- Toth Z, Kalnay E (1993) Ensemble forecasting at NMC: The generation of perturbations. *Bull Amer Meteor Soc* 74: 2317-2330
- Tracton MS, Kalnay E (1993) Operational ensemble prediction at the National Meteorological Center. Practical aspects. *Wea Forecast* 8: 379-398
- Wang X, Bishop CH (2003) A comparison of breeding and ensemble transform Kalman filter ensemble forecast schemes. *J Atmos Sci* 60: 1140-1158
- Wei M, Toth Z, Wobus R, Zhu Y, Bishop CH, Wang X (2006) Ensemble transform Kalman filter-based ensemble perturbations in an operational global prediction system at NCEP. *Tellus* 58A, 28-44
- Wei M, Toth Z (2003) A new measure of ensemble performance: perturbation versus error correlation analysis (PECA). *Mon Wea Rev* 131: 1549-1565
- Whitaker JS, Loughe AF (1998) The relationship between ensemble spread and ensemble mean skill. *Mon Wea Rev* 126: 3292-3302
- Wilks DS (1995) *Statistical Methods in the Atmospheric Sciences*. San Diego: Academic Press, 467 pp
- WMO (1992) *Manual on the global data-processing system*. WMO, n° 485, 217 pp
- Zhang Z (1997) *Hurricane ensemble prediction using EOF-based perturbations*. PhD Dissertation, Florida State University, Florida, 173 pp
- Zhang Z, Krishnamurti TN (1999) A perturbation method for hurricane ensemble predictions. *Mon Wea Rev* 127: 447-469
- Zhu H, Thorpe A (2006) Predictability of extratropical cyclones: the influence of initial condition and model uncertainties. *J Atmos Sci* 63: 1483-1497

Figure Captions:

Fig. 1. January 2005 average pattern anomaly correlation for the deterministic (DET, dashed lines with triangles) and the ensemble mean (EM, solid lines) forecasts for experiments OPER (diamonds), TROP (squares), EXT1 (crosses), EXT2 (stars). Values refer to the 500-hPa geopotential height over the regions (a) Northern Hemisphere, (b) Southern Hemisphere, (c) Tropics, (d) South America, and for 850-hPa wind components over Tropics in (e) and (f).

Fig. 2. January 2005 average RMS error of the ensemble mean forecasts (solid lines) and ensemble standard deviation (dashed lines) for experiments OPER (diamonds), TROP (triangles), EXT1 (stars), EXT2 (circles). Values refer to the 500-hPa geopotential height over the regions (a) Northern Hemisphere, (b) Southern Hemisphere, (c) Tropics, (d) South America, and for 850-hPa wind components over Tropics in (e) and (f).

Fig. 3. January 2005 average Brier skill score for experiments OPER, TROP, EXT1 and EXT2. Values have been computed considering the probability intervals according to the number of ensemble members and refer to the 500-hPa geopotential height over the regions (a) Northern Hemisphere, (b) Southern Hemisphere, (c) Tropics, (d) South America, and for 850-hPa wind components over Tropics in (e) and (f).

Fig. 4. January 2005 average reliability (Rel, solid lines) and resolution (Res, dotted lines) contributions to the Brier score for experiments OPER (triangles), TROP (diamonds), EXT1 (crosses) and EXT2 (stars). Values have been computed considering the probability intervals according to the number of ensemble members and refer to the 500-hPa geopotential height over the regions (a) Northern Hemisphere, (b) Southern Hemisphere, (c) Tropics, (d) South America, and for 850-hPa wind components over Tropics in (e) and (f).

Fig. 5. January 2005 average correlation between control forecast error and ensemble perturbations for experiments OPER (solid lines), TROP (dashed lines), EXT1 (dotted lines) and EXT2 (dash dotted lines). Thin lines represent values averaged over 14 individual ensemble perturbations (sin) while thick lines represent values for an optimal combination of the individual perturbations (opt). Values refer to the 500-hPa geopotential height over the regions (a) Northern Hemisphere, (b) Southern Hemisphere, (c) Tropics and (d) South America.

Fig. 6. January 2005 average correlation between control forecast error and ensemble perturbations for experiments OPER (solid lines), TROP (dashed lines), EXT1 (dotted lines) and EXT2 (dash dotted lines). Thin lines represent values averaged over 14 individual ensemble perturbations (sin) while thick lines represent values for an optimal combination of the individual perturbations (opt). Values refer to the multivariable three-dimensional field (U, V, T at 250, 500 and 850 hPa) over the regions (a) Northern Hemisphere, (b) Southern Hemisphere, (c) Tropics and (d) South America.

Fig. 7. As in Fig. 1 but for experiments ETSA (diamonds), LNGR (crosses) and BRCP (stars).

Fig. 8. As in Fig. 2 but for experiments ETSA (diamonds), LNGR (triangles) and BRCP (stars).

Fig. 9. As in Fig. 3 but for experiments ETSA, LNGR and BRCP.

Fig. 10. As in Fig. 4 but for experiments ETSA (triangles), LNGR (diamonds) and BRCP (crosses).

Fig. 11. As in Fig. 5 but for experiments ETSA (solid lines), LNGR (dashed lines) and BRCP (dotted lines).

Fig. 12. As in Fig. 6 but for experiments ETSA (solid lines), LNGR (dashed lines) and BRCP (dotted lines).

Fig. 13. Relative selecting frequency of the modes 1 to 4 for each analysis perturbed field in experiment LNGR. The values represent a sum over all 31 days used in this study and the five perturbed regions used in experiment LNGR.

Fig. 14. Satellite image from GOES-12 Infrared channel at 13:39 UTC 26th March 2004. It can be seen the well configured hurricane Catarina eye near to Brazilian Coast. From: Environmental Satellite Division - Center for Environmental Prediction - National Institute for Space Research (DSA/CPTEC/INPE).

Fig. 15. Mean sea level pressure (hPa) (contours) and wind speed (m/s) (shaded) fields over Catarina region for the CPTEC-MCGA initial condition at 1200 UTC 24 March 2004. The cyclone central pressure is about 1008 hPa and higher wind speed on the system neighborhood is about 14 m/s.

Fig. 16. Catarina cyclone track as seen by CPTEC-AGCM analyses at T126L28 resolution. The cyclone position is plotted for each 12 hours. The most northern point represents the initial of the trajectory at 1200 UTC 20 March 2004 and the last point (over continent) corresponds to the final position at 1200 UTC 28 March 2004.

Fig.17. Catarina track prediction, starting from 1200 UTC 24 March 2004. The tracks are over four days and positions are plotted for each 12-hours. Trajectories is based on CPTEC-MCGA analyses (solid lines), control forecast (dashed lines), ensemble mean (dotted lines) and individual ensemble members (dots). The panels refer to experiments (a) OPER, (b) TROP, (c) EXT1, (d) EXT2, (e) ETSA, (f) LNGR and (g) BRCP.

Fig.18. Catarina central pressure, starting from 1200 UTC 24 March 2004, as a function of time (in hours) based on CPTEC-AGCM analyses (solid lines), control forecast (dashed lines), ensemble mean (dotted lines) and individual ensemble members (dots). The panels refer to experiments (a) OPER, (b) TROP, (c) EXT1, (d) EXT2, (e) ETSA, (f) LNGR and (g) BRCP.

Mailing address:

Antônio Marcos Mendonça: mendonca@cptec.inpe.br

Instituto Nacional de Pesquisas Espaciais

Rod. Presidente Dutra, Km 40

CPTEC/INPE

Cachoeira Paulista, SP

CEP: 12630-000

Brazil

Tables:

Table 1. Standard deviation value used to rescale the perturbation of specific humidity fields, for each sigma level (σ) of CPTEC-AGCM. The values are multiplied by a factor of 10^3 .

σ	<i>std</i>	σ	<i>std</i>	σ	<i>std</i>	σ	<i>std</i>
1	0.77	8	0.98	15	0.90	22	0.00
2	0.78	9	1.14	16	0.75	23	0.00
3	0.78	10	1.27	17	0.49	24	0.00
4	0.78	11	1.37	18	0.26	25	0.00
5	0.80	12	1.35	19	0.12	26	0.00
6	0.82	13	1.18	20	0.05	27	0.00
7	0.88	14	1.05	21	0.02	28	0.00

Table 2. List of experiments performed and their main characteristics: regions used to compute the perturbations, perturbed fields and methodology used to select the unstable modes.

<i>Experiment</i>	<i>Regions used to compute perturbations</i>	<i>Perturbed fields</i>	<i>Unstable modes selecting methodology</i>
<i>OPER</i>	TRE	T,U,V	mode 1
<i>EXT1</i>	NH,SH,TR	T,U,V	mode 1
<i>TROP</i>	TRE	P,T,Q,U,V	mode 1
<i>EXT2</i>	NH,SH,TR	P,T,Q,U,V	mode 1
<i>ETSA</i>	NH,SH,TR,NSA,SSA	P,T,Q,U,V	mode 1
<i>LNGR</i>	NH,SH,TR,NSA,SSA	P,T,Q,U,V	linear growth
<i>BRCP</i>	GLOBAL	P,T,Q,U,V	breeding

Table 3. Differences between average statistical indexes from experiments ETSA and EXT2 for each forecast lead time. These results are associated with indexes evaluated for 500 hPa geopotential height fields over South America.

<i>Lead time</i>	<i>r</i>	<i>rms</i>	<i>spr</i>	<i>bss</i>	<i>rel</i>	<i>res</i>	<i>peca sin</i>	<i>peca opt</i>	<i>peca3d sin</i>	<i>peca3d opt</i>
1	0.000	0.524	-0.163	-0.026	0.003	-0.004	0.034	-0.042	0.007	-0.033
2	0.000	-0.057	-0.129	0.018	-0.001	0.003	0.006	-0.059	0.023	0.010
3	-0.002	0.162	-0.041	0.032	-0.001	0.006	-0.020	-0.018	0.013	-0.001
4	-0.001	-0.033	0.043	0.026	-0.002	0.004	0.002	-0.016	0.008	-0.004
5	0.000	-0.125	0.073	0.014	-0.002	0.002	0.010	-0.003	0.010	0.009
6	0.002	-0.271	0.164	0.015	-0.001	0.002	0.014	0.008	0.014	0.005
7	0.009	-0.428	0.200	0.021	-0.003	0.002	0.014	0.000	0.016	0.013
8	0.014	-0.570	0.122	0.013	-0.001	0.002	0.022	0.062	0.014	0.027
9	0.020	-0.845	0.162	0.036	-0.004	0.005	0.030	0.057	0.014	0.025
10	0.031	-1.344	0.294	0.064	-0.008	0.007	0.041	-0.004	0.019	0.023
11	0.030	-1.374	0.288	0.061	-0.008	0.006	0.034	-0.024	0.018	0.010
12	0.026	-1.140	0.088	0.039	-0.005	0.004	0.026	-0.056	0.013	0.003
13	0.011	-0.622	-0.147	0.032	-0.004	0.003	0.014	-0.035	0.008	-0.001
14	0.025	-1.240	-0.125	0.053	-0.006	0.006	0.022	0.041	0.007	0.007
15	0.004	-0.604	-0.395	0.042	-0.005	0.005	0.018	0.059	0.004	0.004

Table 4. Differences between average statistical indexes from experiments LNGR and ETSA for each forecast lead time. These results are associated with indexes evaluated for 500 hPa geopotential height fields over South America.

<i>Lead time</i>	<i>r</i>	<i>rms</i>	<i>spr</i>	<i>bss</i>	<i>rel</i>	<i>res</i>	<i>peca sin</i>	<i>peca opt</i>	<i>peca3d sin</i>	<i>peca3d opt</i>
1	0.000	0.021	-0.524	-0.006	0.001	0.000	0.015	0.020	-0.003	-0.014
2	-0.001	0.105	-0.365	-0.005	0.001	0.000	-0.004	0.029	-0.011	-0.023
3	0.000	-0.033	-0.302	-0.007	0.001	-0.001	0.002	0.034	-0.016	-0.026
4	0.000	-0.038	-0.093	-0.005	0.000	-0.001	0.003	-0.039	-0.010	-0.019
5	0.001	-0.146	0.012	-0.025	0.002	-0.004	-0.002	-0.016	-0.004	0.011
6	0.004	-0.270	0.088	-0.009	0.002	-0.001	0.004	0.038	-0.001	0.031
7	0.006	-0.590	0.159	0.006	0.000	0.001	0.020	0.063	0.002	0.025
8	0.010	-0.798	0.240	0.014	-0.001	0.002	0.031	0.011	0.008	0.010
9	0.019	-0.462	0.172	0.000	0.000	0.000	0.008	0.042	0.010	0.007
10	0.026	-0.854	-0.069	-0.017	0.001	-0.003	0.008	0.048	0.004	0.001
11	0.025	-0.713	-0.528	-0.022	0.003	-0.003	0.010	0.054	0.004	-0.007
12	0.015	-0.402	-0.890	0.005	0.001	0.002	0.011	0.048	0.016	-0.003
13	0.003	-0.383	-0.512	0.019	-0.001	0.003	-0.001	-0.014	0.013	-0.002
14	-0.031	0.457	-0.192	-0.011	0.002	-0.001	-0.014	0.006	-0.001	-0.008
15	-0.007	-0.364	0.200	-0.010	0.003	0.000	0.003	0.018	0.000	0.010

Figures:

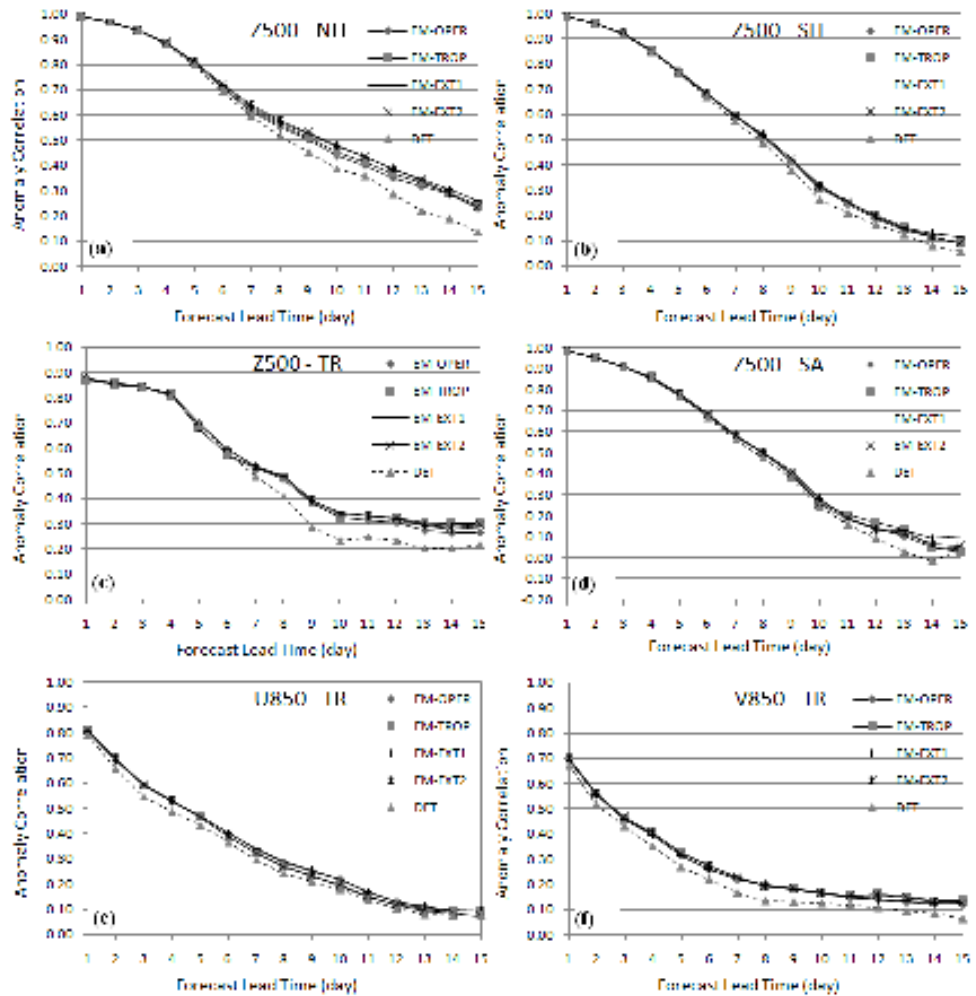


Fig. 1. January 2005 average pattern anomaly correlation for the deterministic (DET, dashed lines with triangles) and the ensemble mean (EM, solid lines) forecasts for experiments OPER (diamonds), TROP (squares), EXT1 (crosses), EXT2 (stars). Values refer to the 500-hPa geopotential height over the regions (a) Northern Hemisphere, (b) Southern Hemisphere, (c) Tropics, (d) South America, and for 850-hPa wind components over Tropics in (e) and (f).

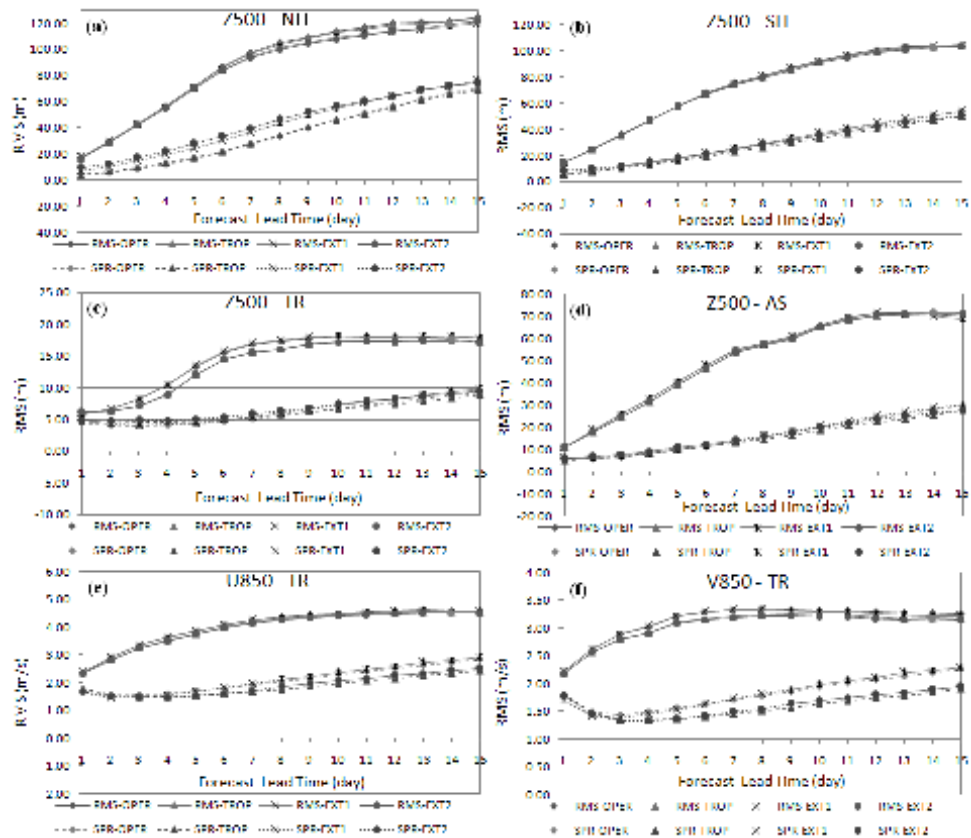


Fig. 2. January 2005 average RMS error of the ensemble mean forecasts (solid lines) and ensemble standard deviation (dashed lines) for experiments OPER (diamonds), TROP (triangles), EXT1 (stars), EXT2 (circles). Values refer to the 500-hPa geopotential height over the regions (a) Northern Hemisphere, (b) Southern Hemisphere, (c) Tropics, (d) South America, and for 850-hPa wind components over Tropics in (e) and (f).

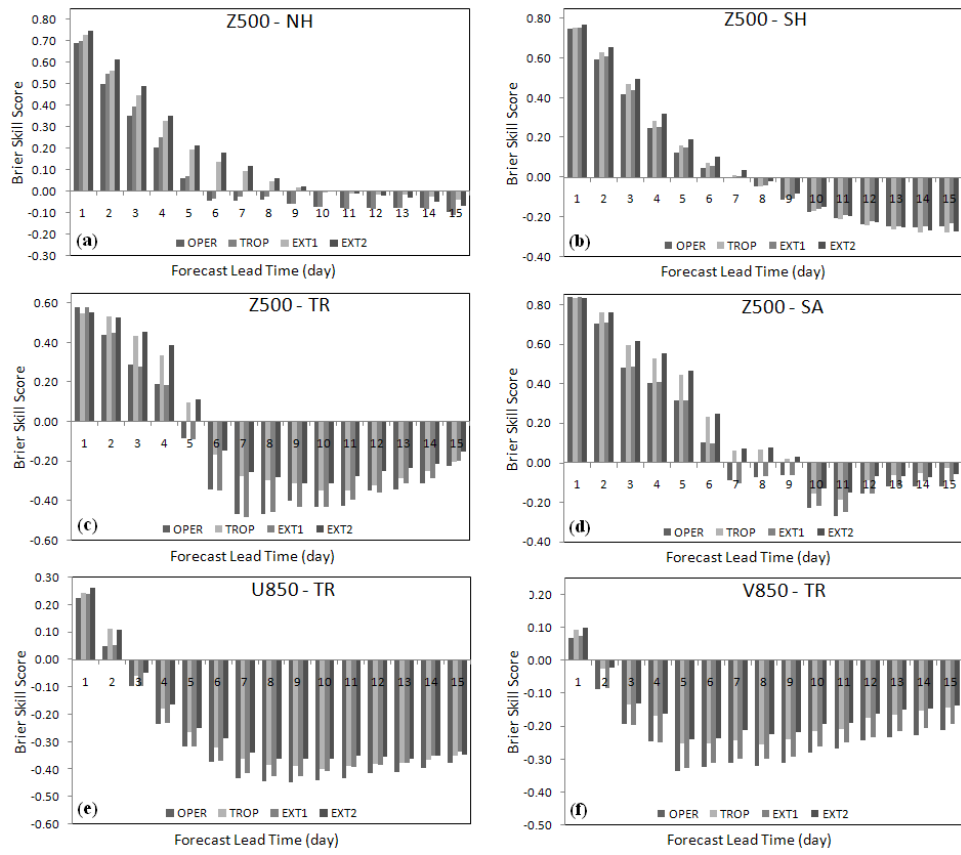


Fig. 3. January 2005 average Brier skill score for experiments OPER, TROP, EXT1 and EXT2. Values have been computed considering the probability intervals according to the number of ensemble members and refer to the 500-hPa geopotential height over the regions (a) Northern Hemisphere, (b) Southern Hemisphere, (c) Tropics, (d) South America, and for 850-hPa wind components over Tropics in (e) and (f).

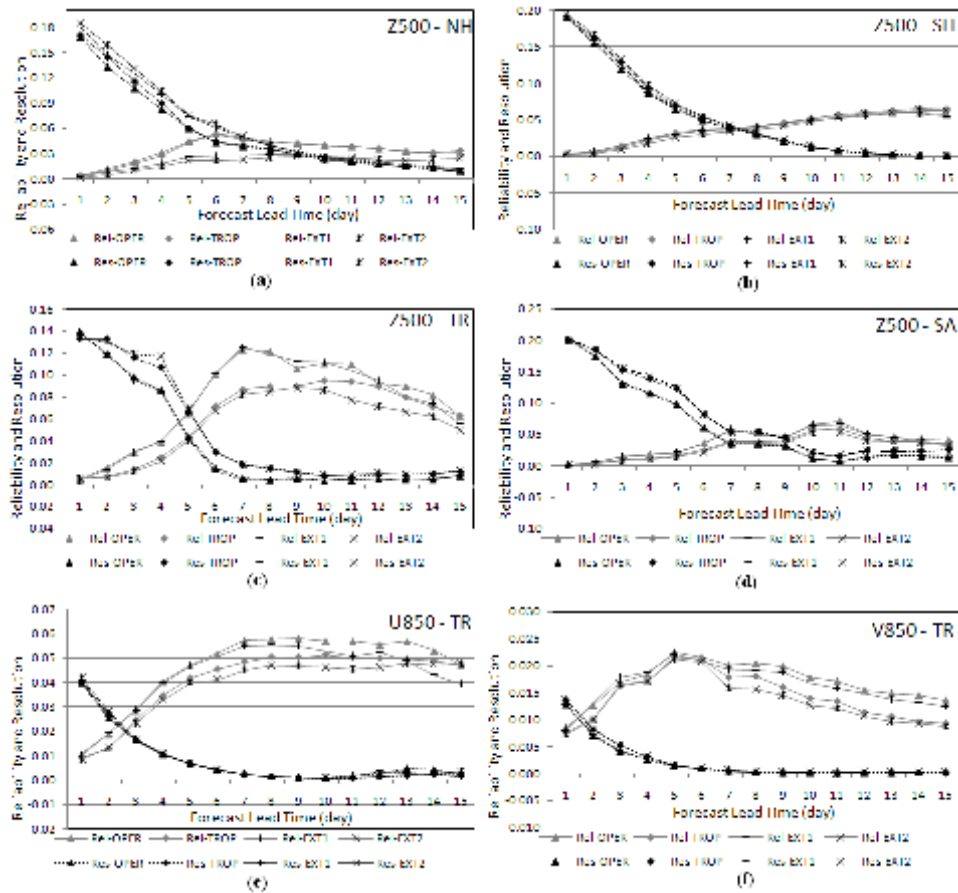


Fig. 4. January 2005 average reliability (Rel, solid lines) and resolution (Res, dotted lines) contributions to the Brier score for experiments OPER (triangles), TROP (diamonds), EXT1(crosses) and EXT2 (stars). Values have been computed considering the probability intervals according to the number of ensemble members and refer to the 500-hPa geopotential height over the regions (a) Northern Hemisphere, (b) Southern Hemisphere, (c) Tropics, (d) South America, and for 850-hPa wind components over Tropics in (e) and (f).

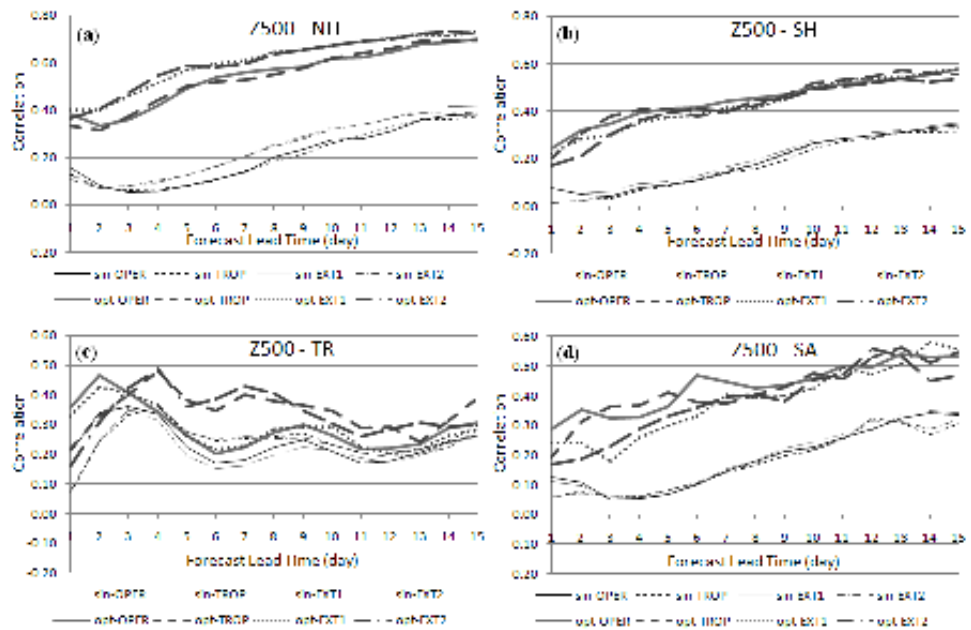


Fig. 5. January 2005 average correlation between control forecast error and ensemble perturbations for experiments OPER (solid lines), TROP (dashed lines), EXT1 (dotted lines) and EXT2 (dash dotted lines). Thin lines represent values averaged over 14 individual ensemble perturbations (sin) while thick lines represent values for an optimal combination of the individual perturbations (opt). Values refer to the 500-hPa geopotential height over the regions (a) Northern Hemisphere, (b) Southern Hemisphere, (c) Tropics and (d) South America.

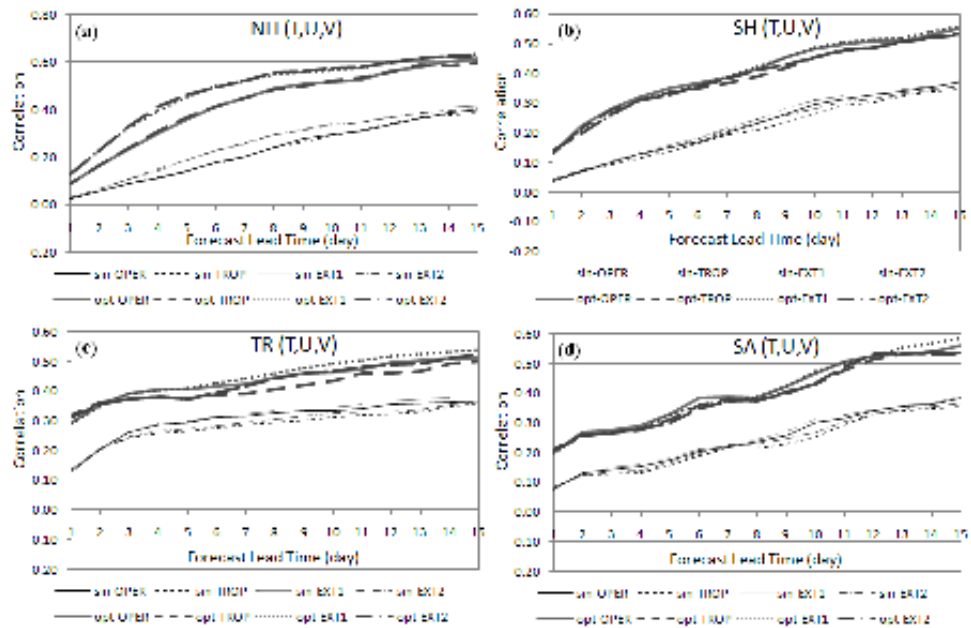


Fig. 6. January 2005 average correlation between control forecast error and ensemble perturbations for experiments OPER (solid lines), TROP (dashed lines), EXT1 (dotted lines) and EXT2 (dash dotted lines). Thin lines represent values averaged over 14 individual ensemble perturbations (sin) while thick lines represent values for an optimal combination of the individual perturbations (opt). Values refer to the multivariable three-dimensional field (U, V, T at 250, 500 and 850 hPa) over the regions (a) Northern Hemisphere, (b) Southern Hemisphere, (c) Tropics and (d) South America.

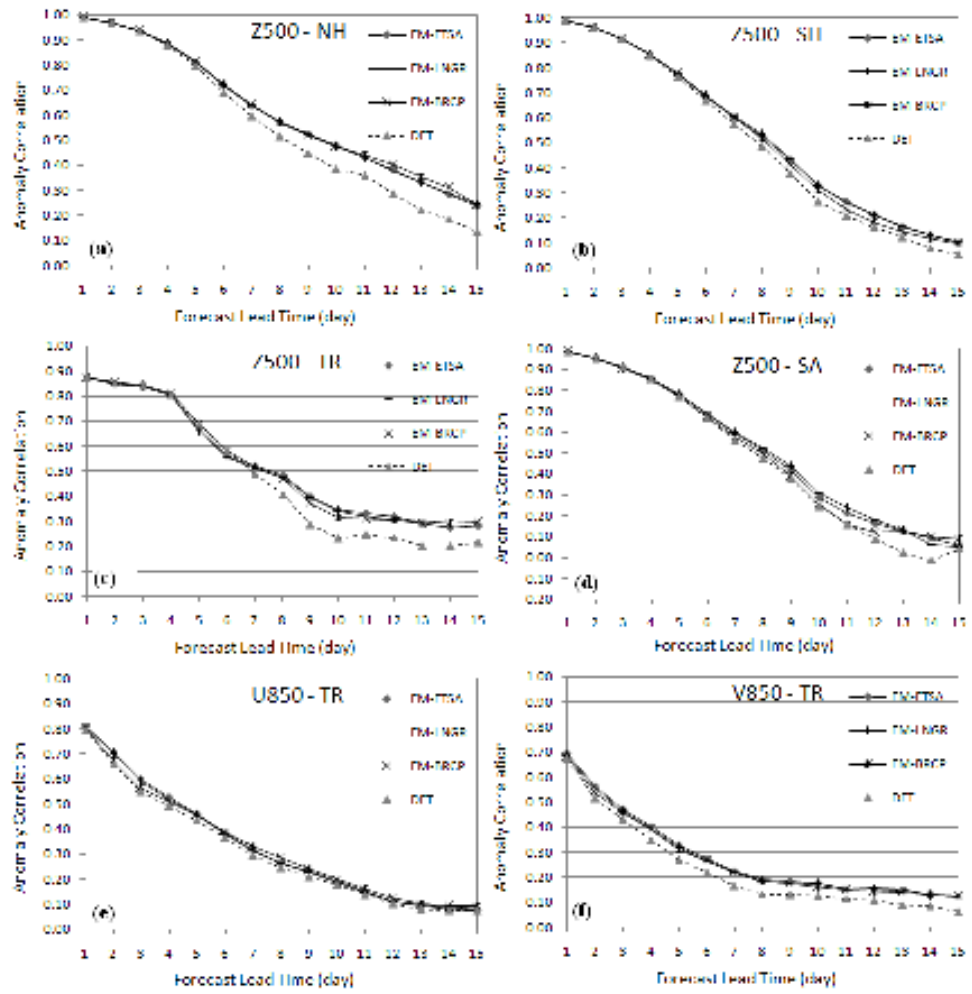


Fig. 7. As in Fig. 1 but for experiments ETSA (diamonds), LNGR (crosses) and BRCP (stars).

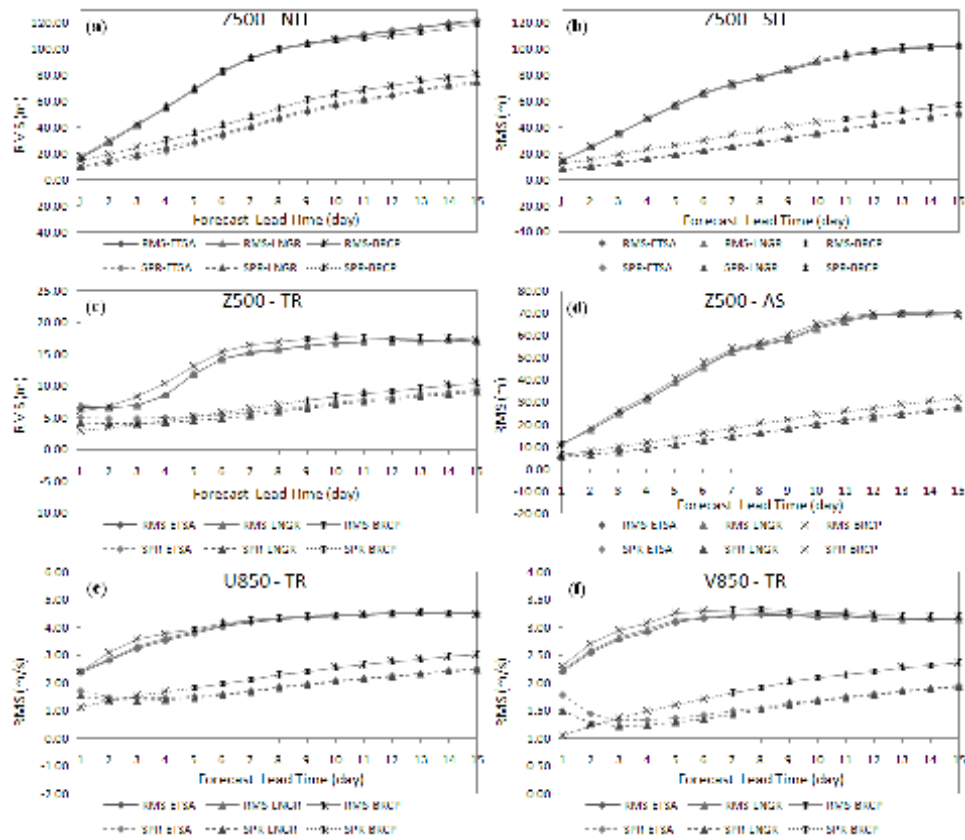


Fig. 8. As in Fig. 2 but for experiments ETSA (diamonds), LNGR (triangles) and BRCP (stars).

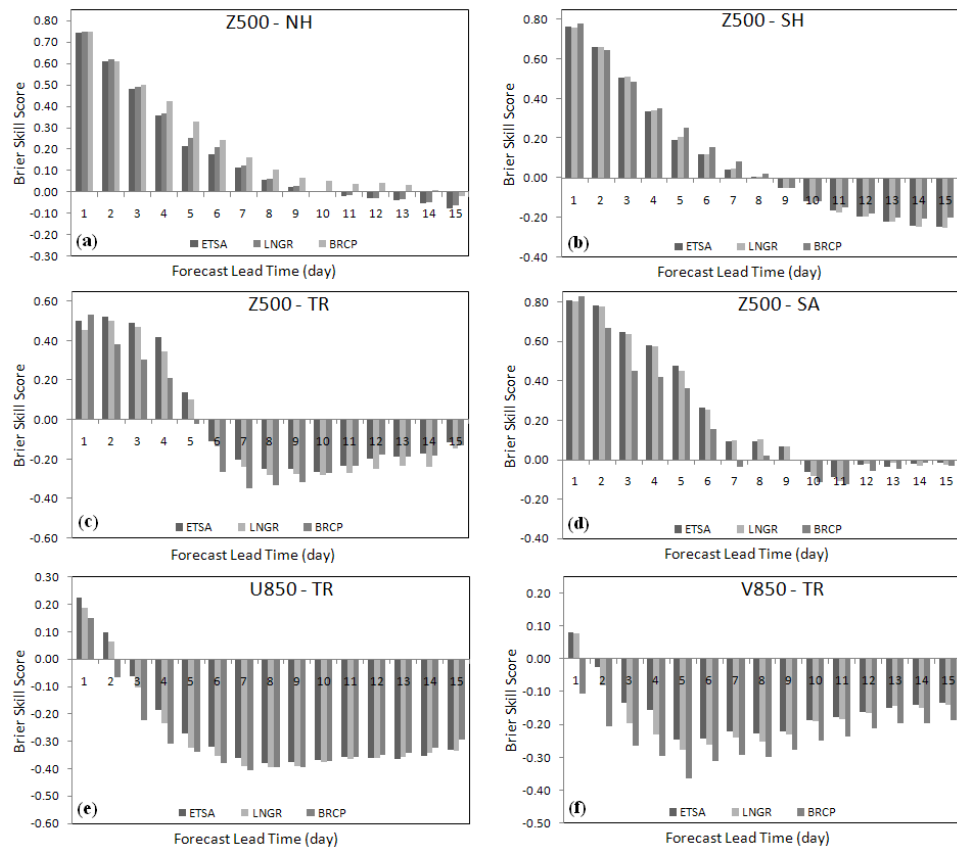


Fig. 9. As in Fig. 3 but for experiments ETSA, LNGR and BRCP.

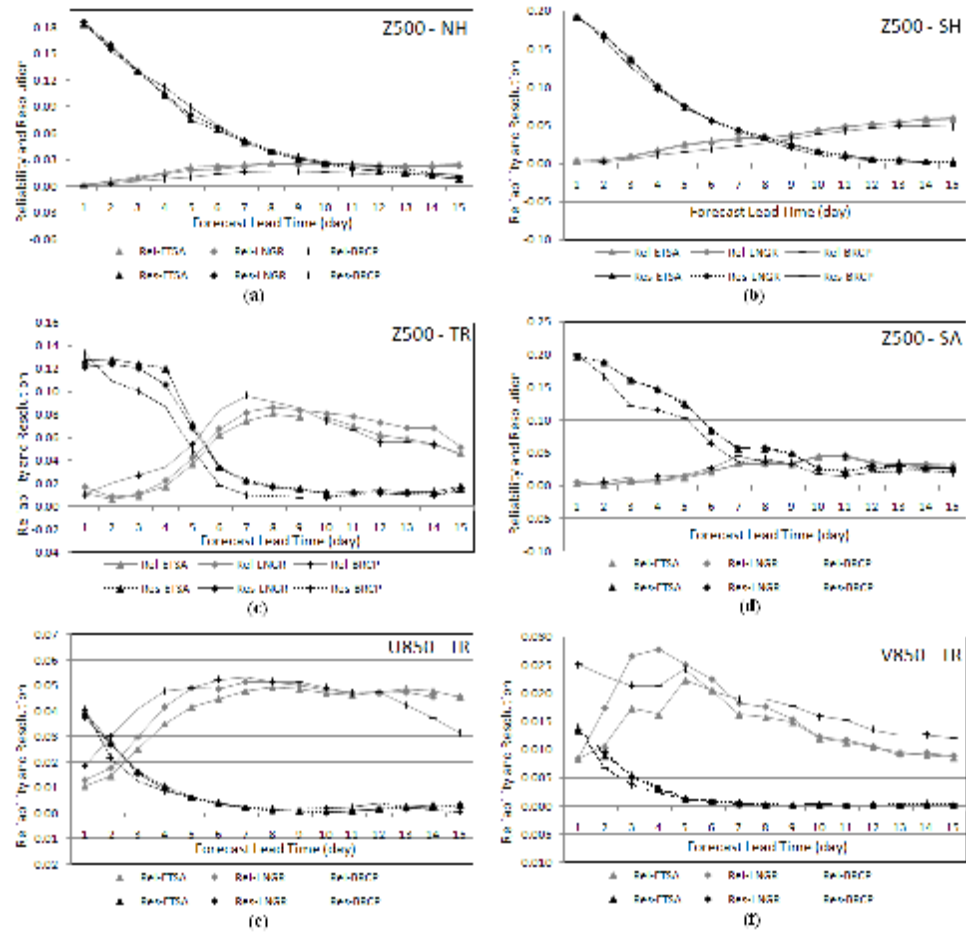


Fig. 10. As in Fig. 4 but for experiments ETSA (triangles), LNGR (diamonds) and BRCP (crosses).

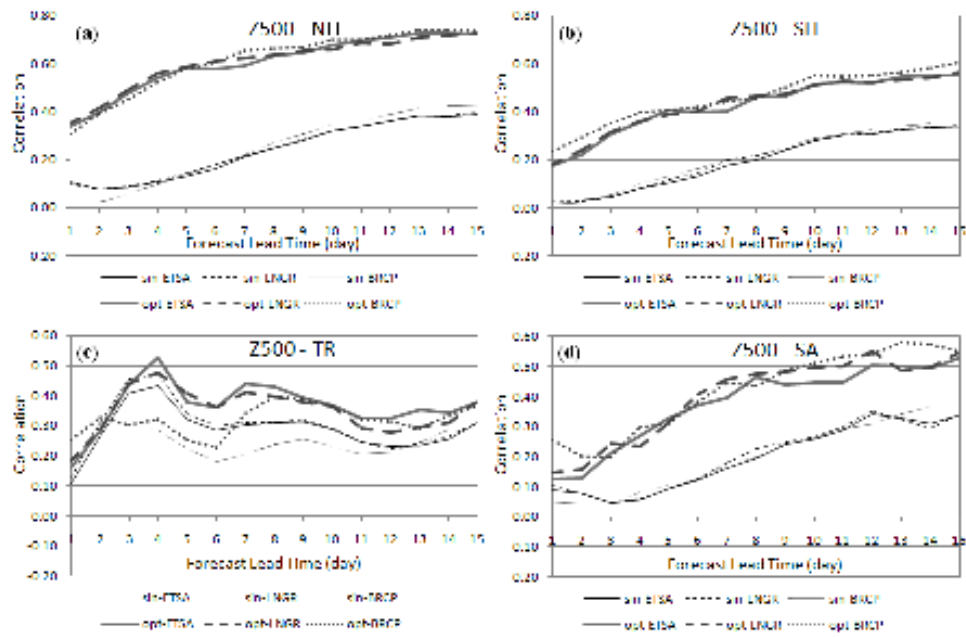


Fig. 11. As in Fig. 5 but for experiments ETSA (solid lines), LNGR (dashed lines) and BRCP (dotted lines).

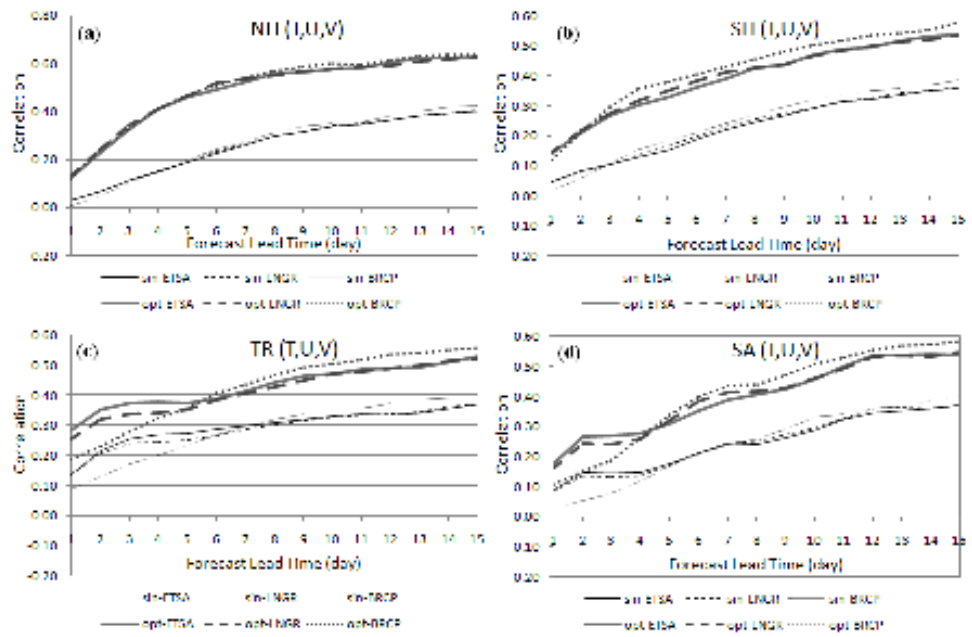


Fig. 12. As in Fig. 6 but for experiments ETSA (solid lines), LNGR (dashed lines) and BRCP (dotted lines).

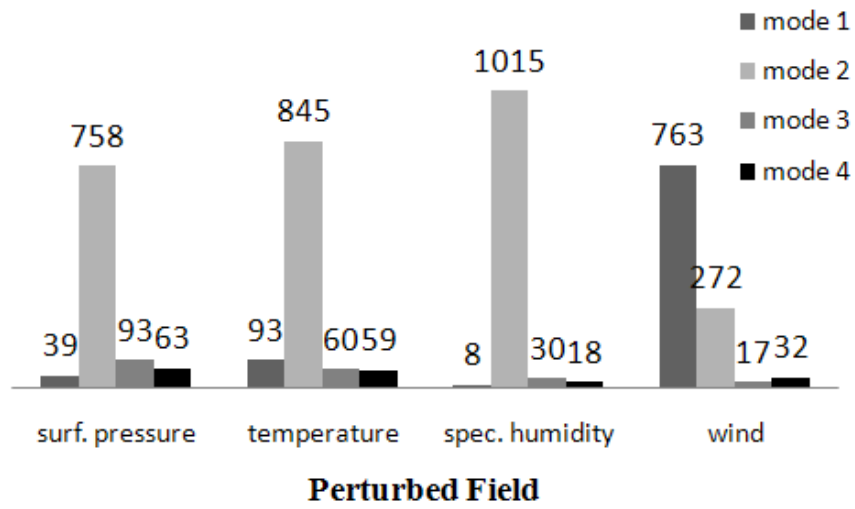


Fig. 13. Relative selecting frequency of the modes 1 to 4 for each analysis perturbed field in experiment LNGR. The values represent a sum over all 31 days used in this study and the five perturbed regions used in experiment LNGR.

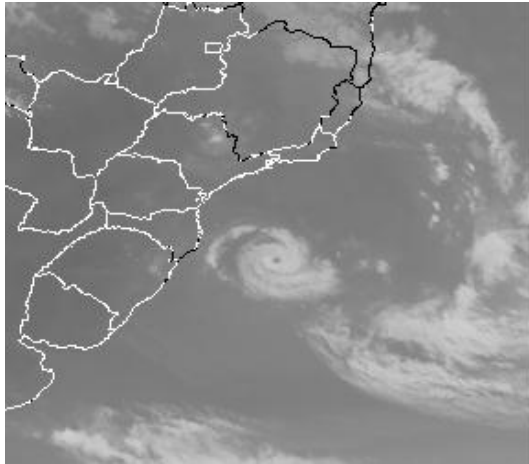


Fig. 14. Satellite image from GOES-12 Infrared channel at 13:39 UTC 26th March 2004. It can be seen the well configured hurricane Catarina eye near to Brazilian Coast. From: Environmental Satellite Division - Center for Environmental Prediction - National Institute for Space Research (DSA/CPTEC/INPE).

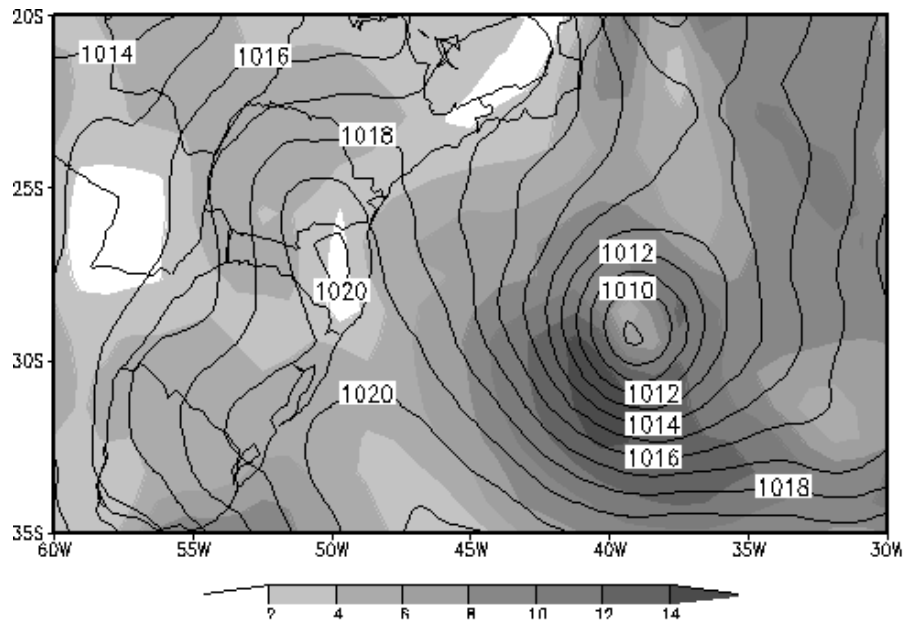


Fig. 15. Mean sea level pressure (hPa) (contours) and wind speed (m/s) (shaded) fields over Catarina region for the CPTEC-MCGA initial condition at 1200 UTC 24 March 2004. The cyclone central pressure is about 1008 hPa and higher wind speed on the system neighborhood is about 14 m/s.

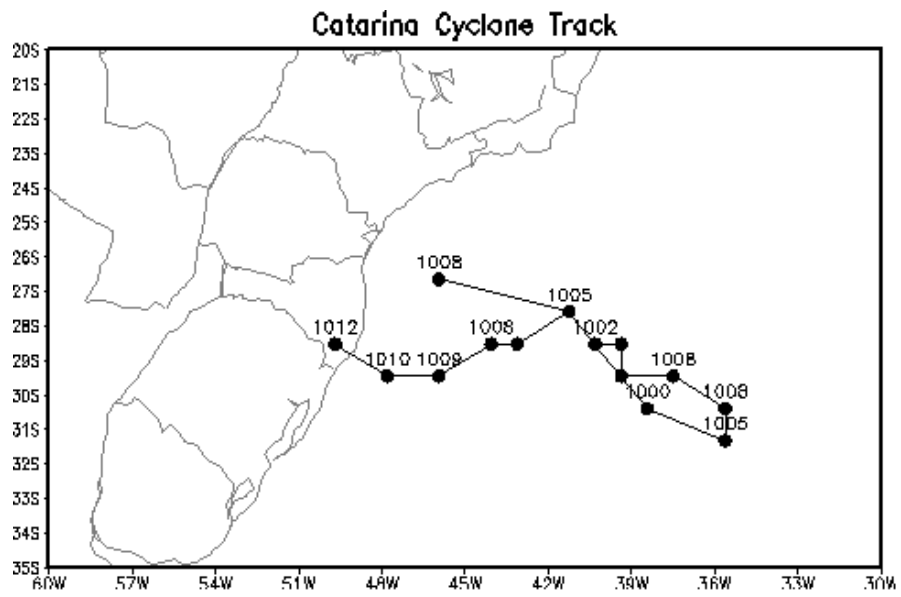


Fig. 16. Catarina cyclone track as seen by CPTEC-AGCM analyses at T126L28 resolution. The cyclone position is plotted for each 12 hours. The most northern point represents the initial of the trajectory at 1200 UTC 20 March 2004 and the last point (over continent) corresponds to the final position at 1200 UTC 28 March 2004.

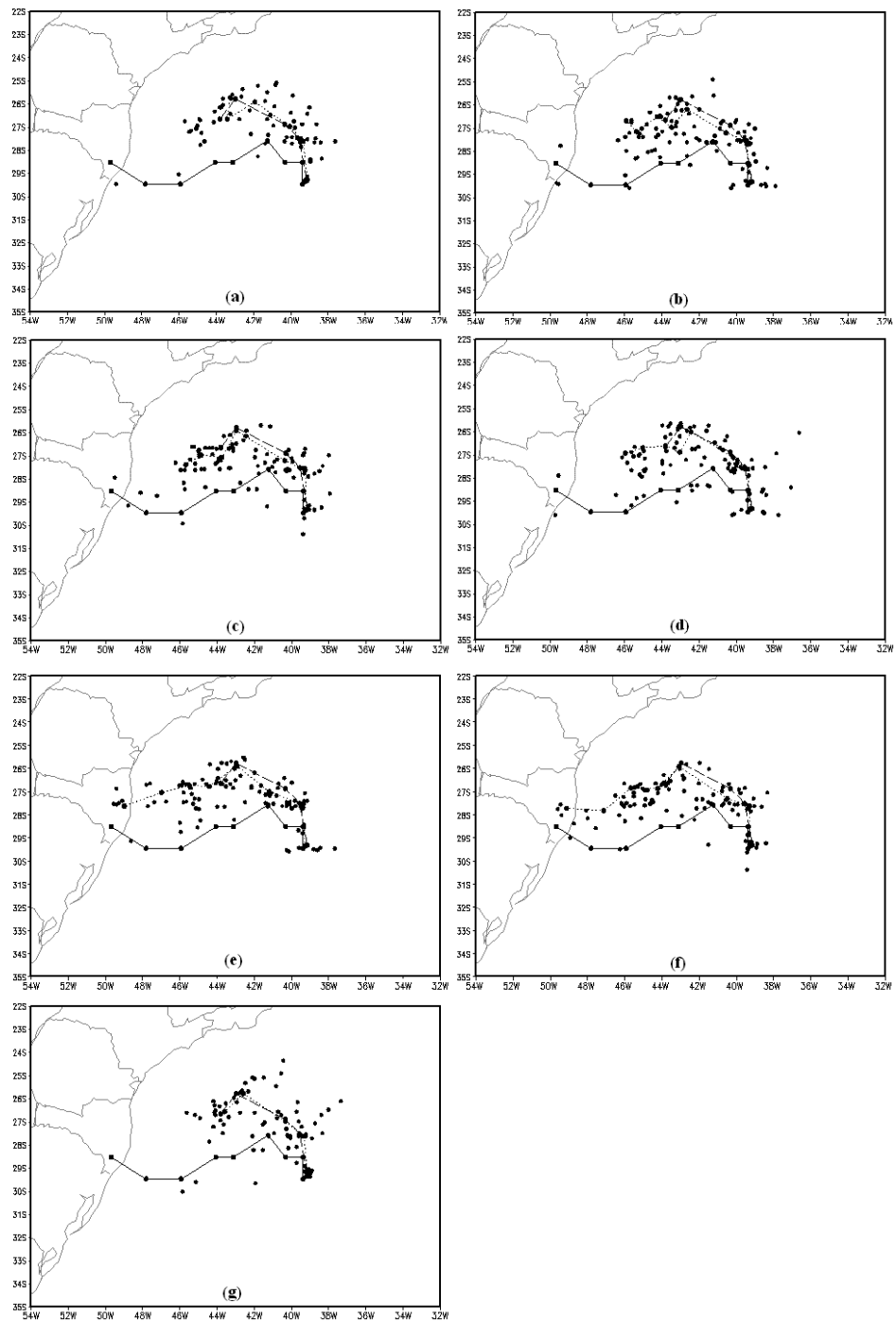


Fig.17. Catarina track prediction, starting from 1200 UTC 24 March 2004. The tracks are over four days and positions are plotted for each 12-hours. Trajectories is based on CPTEC-MCGA analyses (solid lines), control forecast (dashed lines), ensemble mean (dotted lines) and individual ensemble members (dots). The panels refer to experiments (a) OPER, (b) TROP, (c) EXT1, (d) EXT2, (e) ETSA, (f) LNGR and (g) BRCP.

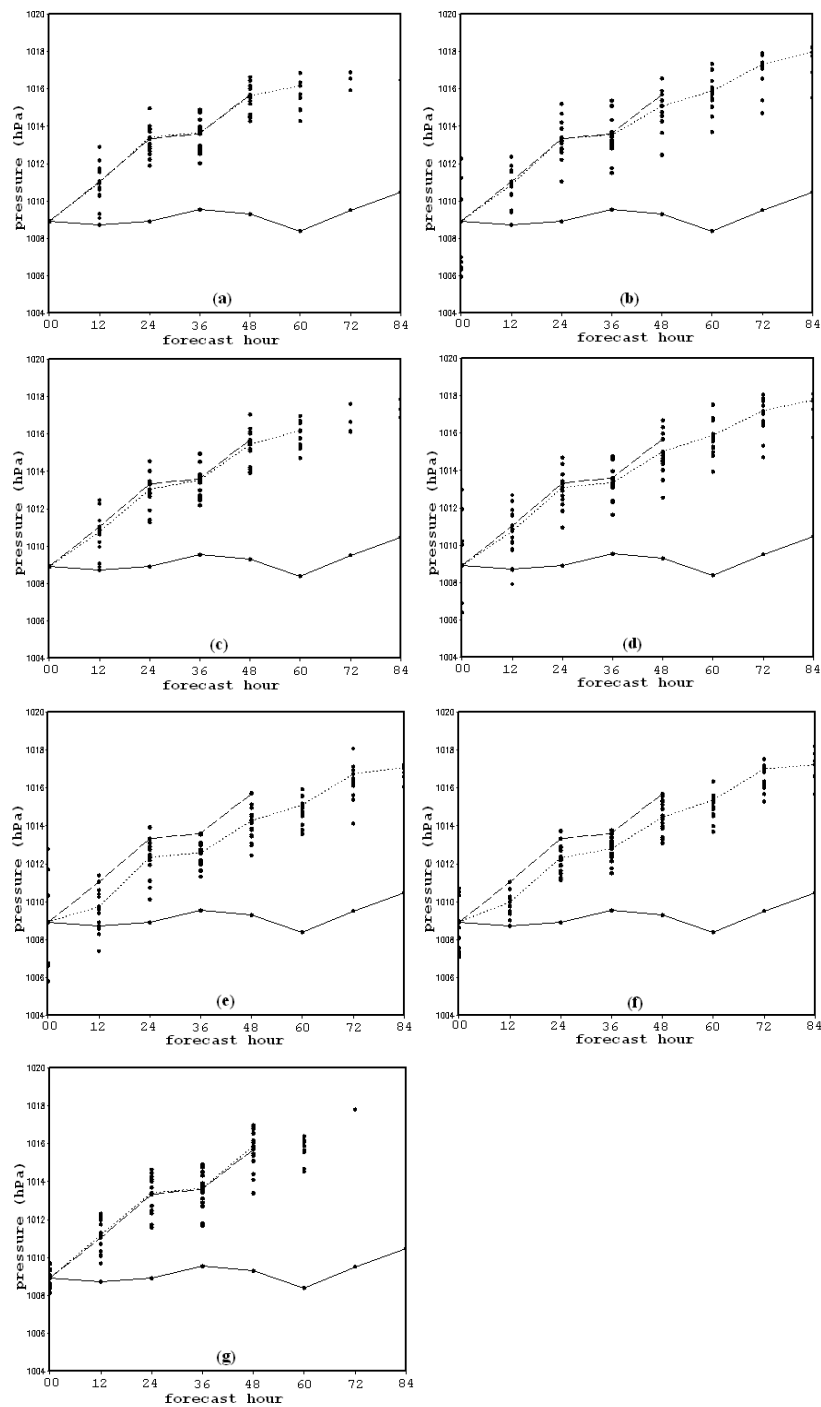


Fig.18. Catarina central pressure, starting from 1200 UTC 24 March 2004, as a function of time (in hours) based on CPTEC-AGCM analyses (solid lines), control forecast (dashed lines), ensemble mean (dotted lines) and individual ensemble members (dots). The panels refer to experiments (a) OPER, (b) TROP, (c) EXT1, (d) EXT2, (e) ETSA, (f) LNGR and (g) BRCP.